CONVENTIONS

SCIENCES DE LA MER

OCÉANOGRAPHIE PHYSIQUE

N° 7

2001

Contribution à l'étude de la variabilité climatique de l'Océan Pacifique tropical sud ouest

Thierry DELCROIX
Yves GOURIOU
Fraçois MASIA
David VARILLON

Institut de recherche pour le développement

Centre de Nouméa

Institut de recherche pour le développement

CONVENTIONS

SCIENCES DE LA MER

OCÉANOGRAPHIE PHYSIQUE

N° 7

2001

Contribution à l'étude de la variabilité climatique de l'Océan Pacifique tropical sud ouest

Thierry DELCROIX
Yves GOURIOU
Fraçois MASIA
David VARILLON

Compte rendu de fin d'étude d'une recherche financée
par le Fond d'Investissement pour le Développement Économique
et Social des Territoires d'Outre mer (FIDES).
Contrat n°99T06, financement 2488.00

Institut de recherche
pour le développement

/Delcroix, T.
/Gouriou, Y.
/Masia, F.
/Varillon, D.

Contribution à l'étude de la variabilité climatique de l'Océan Pacifique tropical sud ouest

Nouméa : IRD. Decembre 2001. 56 p.
Conventions : Sci. Mer ; Océanogr. Phys. ; 7

HYDROCLIMAT ; EL NINO ; VARIABILITE SAISONNIAIRE ; APPAREIL DE MESURE ; PREVISION CLIMATIQUE ; ZONE TROPICALE/OCEAN PACIFIQUE SUD OUEST

Imprimé par la Service de Reprographie
Centre IRD de Nouméa
Décembre 2001

1. INTRODUCTION

Observer et comprendre le climat mais aussi pouvoir anticiper suffisamment à l'avance ses anomalies constituent des enjeux scientifiques, techniques et socio-économiques incontestables. Le phénomène El Niño Southern Oscillation (ENSO) est le signal climatique qui domine à l'échelle interannuelle dans le Pacifique tropical. L'analyse d'observations *in situ* et altimétriques ainsi que les résultats de modèles ont permis ces dernières années de suivre certains phénomènes en temps réel et de les prévoir environ 6 mois en avance. En dépit de ce succès relatif, notre compréhension d'ENSO demeure incomplète, liée en partie aux manques d'observations sur l'océan.

Le Pacifique tropical sud-ouest est une région d'intérêts multiples à la fois scientifiques et socio-économiques. Cette région englobe une grande partie du réservoir d'eau chaude du Pacifique où se trouvent les eaux les plus chaudes de la planète (>28°C). Elle est également située entre les deux systèmes météorologiques du Pacifique qui définissent l'indice d'Oscillation Australe (Tahiti et Darwin) et cette position géographique unique a suggéré à certains auteurs que l'origine d'ENSO devait y être recherchée (Van Loon and Shea, 1985; Holbrook and Bindoff, 1997). En dehors de l'aspect strictement scientifique, cette région comprend les TOM (Territoires d'Outre Mer) Français et de nombreux Etats Insulaires et Territoires, membres du Programme Régional Océanien de l'Environnement (PROE), désireux de connaître leur environnement climatique et ses modifications passées, présentes et futures.

Les deux grands traits caractéristiques de la région sont l'existence de la Zone de Convergence du Pacifique Sud (SPCZ; cf. Vincent, 1994) et du grand tourbillon anticyclonique qui recouvre l'ensemble du Pacifique sud. La SPCZ est associée à des précipitations très importantes (de 2 à 6 m/an; e.g., Delcroix et al., 1996) et le grand tourbillon à une circulation océanique vers l'est au sud d'environ 15°S et vers l'ouest au nord de cette latitude. En période El Niño, la SPCZ se déplace vers l'équateur et l'axe du grand tourbillon se déplace de quelques centaines de kilomètres vers le sud (Wyrtki et Wenzel, 1984; Delcroix et Hénin, 1989). Des déplacements inverses sont observés en période La Niña. Les déplacements méridiens de la SPCZ et du grand tourbillon entraînent de fortes anomalies atmosphériques et océaniques, en particulier ils modifient de manière fondamentale la pluviométrie régionale, la salinité, le niveau de la mer et la circulation océanique avec renverse possible des courants zonaux. Nous savons

maintenant, sans toutefois en comprendre pleinement les mécanismes, que les anomalies ENSO observées dans les TOM du Pacifique tropical sud-ouest peuvent être de signes contraires aux anomalies de la bande équatoriale (Delcroix et Lenormand, 1997; Delcroix, 1998; Alory et Delcroix, 1999 ; Nicet et Delcroix, 2000).

Le maintien et la mise en place d'observatoires du milieu océanique sont nécessaires pour comprendre et aboutir à terme à une prévision opérationnelle d'ENSO, en particulier au voisinage des TOM du Pacifique directement affectés par le phénomène. Dans ce cadre, la proposition financée par le FIDES en 2000-2001 visait à améliorer l'observation et la compréhension de la variabilité climatique à l'échelle régionale, en priorité à l'échelle d'ENSO mais également à d'autres échelles de temps. Quatre types de travaux ont été effectués:

- Le maintien d'un thermosalinographe (mesurant la température et la salinité) dans le lagon de l'île de Wallis,
- la mise en place d'un thermosalinographe sur un navire de commerce faisant une route régulière dans le Pacifique tropical sud-ouest, avec transmission des données en temps réel,
- la mise à disposition via Internet des données récoltées,
- la valorisation scientifique et la publication de résultats liés à l'exploitation des données récoltées.

Ces quatre types de travaux sont décrits tour à tour.

2. TRAVAUX EFFECTUES

2.1. Mise en place d'un thermosalinographe dans le lagon de l'île de Wallis

Un thermosalinographe de type Seabird SBE-21 a été installé prés de la passe de Futumanimi (13°13'334S ; 176°15'094°E) sur l'île de Wallis le 22/08/1998 par 9 m de profondeur (Figure 1). Cet appareil aurait été enlevé sans le soutien financier du FIDES en 2000-2001. Il est programmé pour mesurer et enregistrer la température et la salinité de surface toutes les 30 minutes. La cellule de conductivité permettant de mesurer la salinité est vérifiée tous les 6 mois environ et l'appareil est envoyé chez le fabricant SeaBird (USA) tous les ans pour étalonnage des capteurs. Des prélèvements manuels d'échantillon d'eau de mer sont effectués lors de l'opération de nettoyage des capteurs. Les mesures de température et

salinité de surface n'ont pas encore été exploitées scientifiquement en raison de la longueur encore trop faible des séries temporelles. Les données récoltées sont en cours de validation.

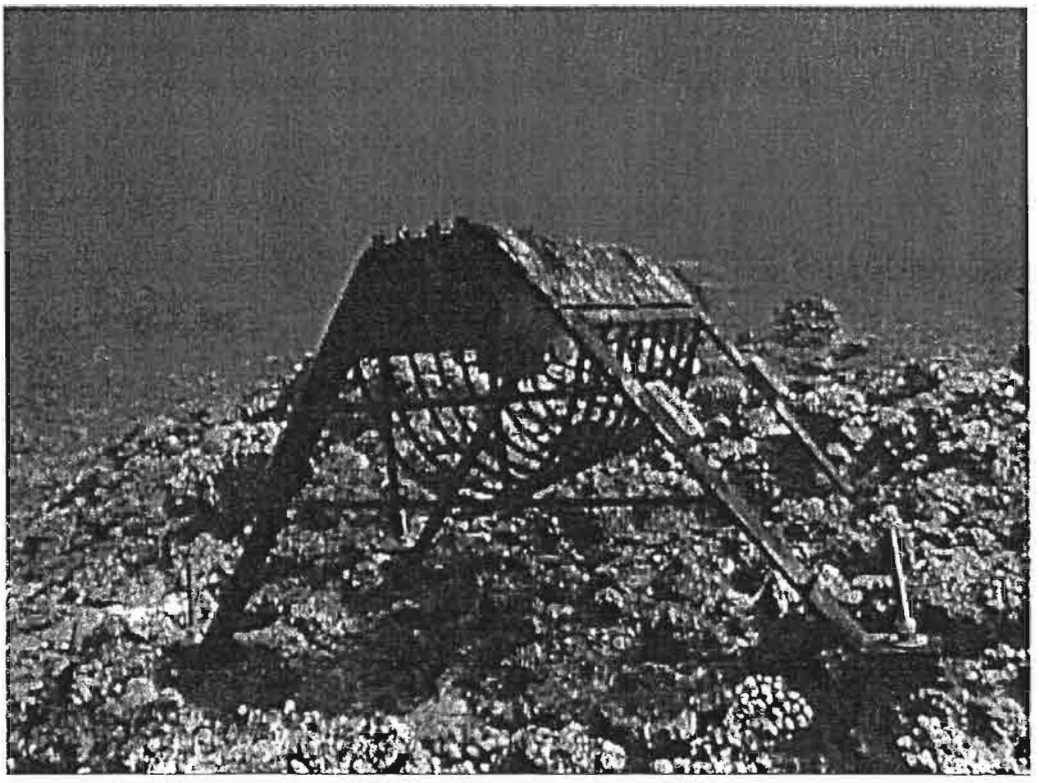

Figure 1. Photographie du thermosalinographe sur son bâti à Wallis.

2.2. Mise en place d'un thermosalinographe sur un navire de commerce

Pour des raisons commerciales, le bateau Moana sur lequel il était prévu d'installer un thermosalinographe (voir proposition initiale) n'a plus effectué de navettes régulières entre Wallis, Fidji et la Nouvelle Calédonie à partir de début 2000. L'installation d'un thermosalinographe a donc été effectuée sur le M/S Kyowa Hibiscus, navire effectuant le même type de trajet avec en plus un aller retour sur le Japon et sur la Polynésie Française (Figure 2). Le schéma de l'installation est décrit en détail dans Prunier-Mignot et al. (1999).

L'appareil installé mesure la température et la salinité de surface toutes les 15 secondes, une médiane est calculée sur 5 minutes, ces valeurs médianes sont stockées avec le temps et la position GPS sur le disque dur d'un PC situé à la passerelle, les valeurs médianes calculées sur 1 heure sont transmises en temps réel via le système GOES. La transmission temps réel est conforme aux impératifs des programmes international GODAE et national MERCATOR d'océanographie opérationnelle. Le thermosalinographe est nettoyé avec une

solution de Triton 1% lors de chaque escale à Nouméa et les tuyauteries installées par nos soins, qui relient le système de refroidissement du navire au thermosalinographe, sont changées tous les ans. L'appareil est également envoyé chez le fabricant SeaBird (USA) tous les ans pour étalonnage des capteurs.

Des prélèvements d'eau de mer, au niveau du thermosalinographe, ont été réalisées par les officiers du bord ou par le personnel de la machine, à raison de deux échantillons minimum par jour. Ils visaient à minimiser l'effet de la dérive temporelle des capteurs de salinité, liée à l'encrassage de la cellule, par ajustement des valeurs du thermosalinographe aux valeurs des échantillons. Cette dérive peut être estimée à environ 0.1 psu / mois pour la salinité. Ces tentatives n'ont hélas pas été très fructueuses car de nombreuses mesures issues des échantillons d'eau de mer se sont avérées totalement irréalistes. Ces tentatives doivent être reconduites.

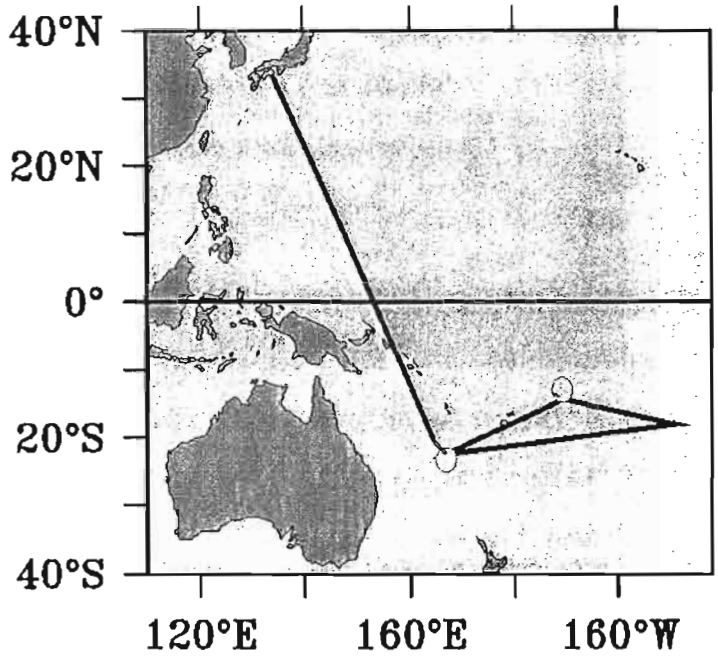

Figure 2. Route type (en noir) du M/S Kyowa Hibiscus sur lequel est installé un thermosalinographe. Les cercles représentent les thermosalinographes mouillés à Wallis et en Nouvelle Calédonie.

2.3. Mise à disposition via Internet des données récoltées

L'installation décrite précédemment vient en réalité compléter un réseau de thermosalinographes installés sur des navires marchands par notre laboratoire depuis le début des années 1990. Ce type de mesures existe sur plusieurs lignes de navigation, actuellement sur 4 lignes Pacifique ouest et 3 lignes tour du monde. L'avantage de cette nouvelle installation financée par le FIDES pour le Pacifique tropical sud-ouest, incluant les TOM français, est de permettre un échantillonnage beaucoup plus fin à la fois dans le temps et dans l'espace de cette région.

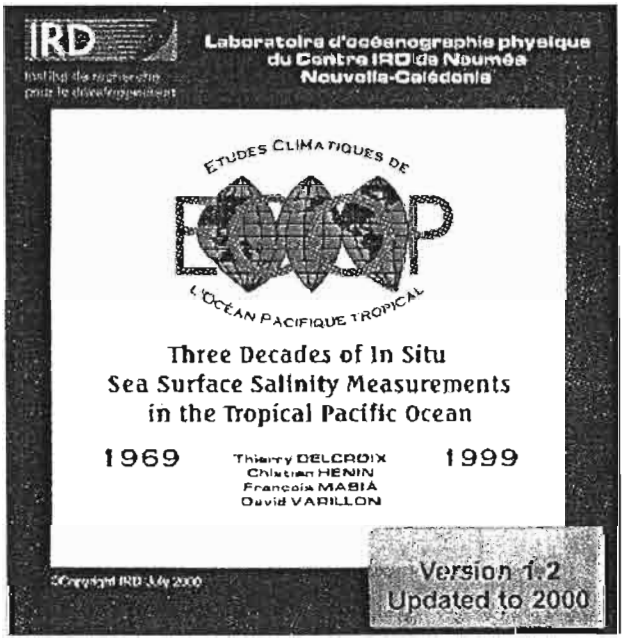

Figure 3. Couverture du CD-ROM rassemblant les mesures de salinité de surface des années 1969 à 2000 dans le Pacifique tropical (version 1.2). Voir aussi http://www.ird.nc/ECOP.

En adéquation avec les objectifs scientifiques du programme international CLIVAR (et avec un financement MERCATOR complémentaire), les mesures récoltées grâce à cette nouvelle installation ont aussi été mises à disposition de la communauté scientifique attachée à l'étude de la variabilité climatique dans le Pacifique tropical. Un CD-ROM rassemblant l'ensemble des mesures de salinité de surface effectuées depuis 1969 dans le Pacifique tropical par l'IRD et par d'autres organismes (IFREMER, NOAA, JAMSTEC, etc...) a donc été réalisé (Figure 3) et diffusé à plus de 200 scientifiques de part le monde. Ce CD-ROM a été mis en accès libre en septembre 2000 via le site Web de notre laboratoire http://www.ird.nc/ECOP.

Le site est réactualisé tous les 6-12 mois avec les données en temps différé qui continuent à être récoltées et validées. Les procédures de validation et les codes de qualité attribués aux données sont décrits dans le CD-ROM.

2.4. Valorisation scientifique et publications

Quatre articles de rang A utilisant les données nouvellement récoltées ont été publiés (ou sous presse) en 2000-2001. Il s'agit :

- D'une étude spécifique sur la variabilité saisonnière et liée à ENSO dans le Pacifique tropical sud ouest sur la période 1976-2000 (Gouriou et Delcroix, 2001).
- D'une étude sur la variabilité de la salinité de surface à Fidji, à la fois avec des mesures directes et en utilisant des données coralliennes (Lebec et al., 2000).
- D'une étude sur la variabilité de la température de surface à Vanuatu dans laquelle la période actuelle est comparée à la période du mid-holocène (Corrège et al., 2000).
- D'une étude sur la variabilité de la température de surface en Nouvelle Calédonie dans laquelle la période actuelle est comparée à la période du petit age glaciaire (Corrège et al., 2001).

Ces quatre articles sont reproduits en Annexe.

REFERENCES

Alory G. et T. Delcroix, 1999. Climatic variability in the vicinity of Wallis, Futuna and Samoa islands (13°S-15°S; 180°-170°W). *Oceano. Acta*, 22, 249-263.

Correge T., T. Delcroix, J. Recy, W. Beck, G. Cabioch et F. Le Cornec, 2000. Evidence for stronger El Niño Southern Oscillation (ENSO) events in a mid-Holocene massive coral. *Paleoceanography*, 15, 465-470.

Correge, T., T. Quinn, T. Delcroix, F. Le Cornec, J. Recy and G. Cabioch, 2001 : Litte Ice Age sea surface temperature variability in the southwest tropical Pacific, *Geophys. Res. Let.*, 28, 3477-3480.

Delcroix T. et C. Hénin, 1989. Mechanisms of subsurface thermal structure and sea surface thermohaline variabilities in the southwestern tropical Pacific during 1979-85. *J. Mar. Res.*, 47, 777-812.

Delcroix T., C. Hénin, V. Porte et P. Arkin, 1996. Precipitation and sea-surface salinity in the tropical Pacific. *Deep Sea Res.*, 43, 1123-1141.

Delcroix T. et O. Lenormand, 1997. ENSO signals in the vicinity of New Caledonia, south-western Pacific. *Oceano. Acta*, 20, 481-491.

Gouriou, Y. et T. Delcroix, 2001. Seasonal and ENSO variations of sea surface salinity and temperature in the South Pacific Convergence Zone during 1976-2000. *J. Geophys. Res.*, in press.

Holbrook, N.J. and N.L. Bindoff, 1997. Temperature variability in the Southwest Pacific Ocean between 1955 and 1988, *J. Climate*, 10,31035-1049.

Le Bec N., A. Juillet-Leclerc, T. Correge, D. Blamart, and T. Delcroix, 2000. A coral $\delta^{18}O$ record of ENSO driven sea surface salinity variability in Fiji (South – Western Tropical Pacific). *Geophys. Res. Letter*, 27, 3897-3900.

Nicet J.B. et T. Delcroix, 2000. ENSO-related precipitation changes in New Caledonia, South Western Tropical Pacific. 1969-1998. *Mon. Wea. Rev.*, 128, 3001-3006.

Prunier-Mignot, M., D. Varillon, L. Foucher, J.-M. Ihily, B. Buisson, F. Masia, C. Hénin, M. Ioualalen and T. Delcroix, 1999. Manuel d'installation et de maintenance d'un thermosalinographe embarqué / Users guide for thermosalinograph installation and maintenance aboard a ship. Notes techniques, Sciences de la Mer, Océanogr. Phys., Centre ORSTOM de Nouméa, 13, 102 pages.

van Loon H. and J. Shea, 1985. The Southern Oscillation. IV. The precursors south of 15°S to the extremes of the Oscillation. *Mon. Weather Rev.*, 113, 2063-2074.

Vincent, D.G., 1994. The South Pacific Convergence Zone (SPCZ): a review, *Mon. Weather Rev., 122*, 1949-1970.

Wyrtki K. and J. Wenzel, 1984. Possible gyre-gyre interaction in the Pacific ocean. *Nature*, 309, 538-540.

Seasonal and ENSO Variations of Sea Surface Salinity and Temperature in the South Pacific Convergence Zone during 1976-2000

Yves Gouriou and Thierry Delcroix

Centre IRD, B.P. A5, 98 848 Noumea, New Caledonia
e.mail : yves.gouriou@noumea.ird.nc

Accepté dans Journal of Geophysical Research

2001#830

October 2001

Index term :
4215 Climate and interannual variability
4223 Descriptive and regional oceanography
4522 El Niño

Key Words : ENSO – Variability - Sea Surface Salinity – Sea Surface Temperature – South Pacific Convergence Zone – Front -

Abstract

Sea surface salinity (SSS) and temperature (SST) data collected from voluntary observing ships over 25 years (1976-2000) are analyzed in the South Western Tropical Pacific (10°S-24°S / 160°E-140°W). This region lies under the South Pacific Convergence Zone (SPCZ), at the southern edge of the western Pacific warm pool, between Tahiti and Darwin the two places whose atmospheric sea level pressure difference is used to define the Southern Oscillation Index (SOI). Complementary data such as precipitation are used to assist in the analysis. The mean and seasonal variations of these parameters are described. An Empirical Orthogonal Function (EOF) analysis of low-pass filtered time-series is then performed to extract the interannual variability. All parameters show an interannual signal which correlates well with the SOI. The South Western Tropical Pacific Ocean is saltier and colder during El Niño than during La Niña events. In the southwestern part, there is a shortage (excess) in precipitation during El Niño (La Niña) events. The greatest anomalies appeared during the last La Niña, in 1996 and 1999 as regards SST and in 1999 and 2000 as regards SSS. SST and precipitation ENSO-related anomalies are an order of magnitude smaller than seasonal anomalies, while the SSS ENSO-related signal is twice as strong as the seasonal signal. These facts reflect the northeastward (southwestward) shift of the SPCZ during El Niño (La Niña) events. While consistent with precipitation changes, the ENSO-related variability in SSS can also be partly explained by the displacement of the salinity front that separates fresh warm pool waters from salty subtropical waters. Computation of surface geostrophic current anomalies from GEOSAT (1987-1988) and TOPEX/Poseidon (1993-2000) indicates that westward current anomalies developed during the 1987/88 and 1997/98 El Niño and are linked to the displacement of the salinity front. The South Western Tropical Pacific salinity front moves westward (eastward) in contrast to the equatorial salinity front which moves eastward (westward) during an El Niño (La Niña) event.

1. Introduction

Recent studies [*Picaut et al.*, 1996, 1997, 2001; *Vialard and Delecluse*, 1998] highlighted the dynamical and biogeochimical importance of the Pacific equatorial frontal zone (~175°W) which separates the warm/fresh pool to the west from the colder and saltier waters to the east (Figure 1). This front is mainly defined by a zonal gradient of Sea Surface Salinity (SSS), whereas Sea Surface Temperature (SST), gradually increasing to 28.5°C from east to west, is relatively constant (Figure 1). These studies particularly stressed the front's relationship with El Niño Southern Oscillation (ENSO) variability, demonstrating that its zonal displacements at an interannual time-scale are mainly due to advection processes rather than to the Evaporation/Precipitation budget.

The climatic importance of the equatorial salinity front led us to look more closely at a second frontal region, located south of the equator (~170°W-15°S), at the southeastern side of the warm pool (Figure 1). This secondary salinity front is the result of the juxtaposition of the high salinity waters formed in the subtropical region (20°S-120°W), where evaporation exceeds precipitation, and of the low-salinity waters of the warm pool area, where precipitation exceeds evaporation. This frontal region is located under the South Pacific Convergence Zone (SPCZ) which plays a significant role in global atmospheric circulation. The SPCZ extends southeastward from Papua New Guinea (~5°S-145°E) to about 30°S-120°W, over southeastward warm-SST, low-SSS (in its western part), and maximum precipitation tongues. The importance of the SPCZ has been brought to light since the advent of satellite imagery, and the use of Outgoing Longwave Radiation (OLR) data as a proxy for deep tropical convection and global circulation. The annual cycle of the SPCZ is thus characterized by high deep convection activity during the austral winter and low deep convection activity during the summer [*Meehl*, 1987; *Vincent*, 1994]. The SPCZ shifts north and east (south and west) of its average position during an El Niño (La Niña) event [*Pazan and Meyers*, 1982; *Vincent*, 1994].

Few previous studies investigated the links between El Niño and La Niña and the interannual variability of oceanic and atmospheric parameters in the South Western Tropical Pacific (SWTP), defined here as the region between 24°S-10°S and 160°E-140°W (Figure 1). *Delcroix and Hénin* [1989] analyzing Voluntary Observing Ship (VOS) data between 1979 and 1985 stressed the influence of the 1982-1983 El Niño event on SST, SSS, and subsurface thermal structure variability. They

particularly noted that SSS increased by +1 in early 1983, mainly in response to a rainfall shortage due to a northward migration of the SPCZ. *Delcroix and Hénin* [1991], studying the 1972-1988 SSS variability along 4 main shipping routes, found that during the warm phases of ENSO, SSS is fresher than average west of 150°W within 8°S-8°N, and saltier than average poleward of 8° latitude (i.e. in the SWTP). *Delcroix et al.* [1996] indicated that the 1974-1989 interannual variations of SSS in the SWTP, are closely related to the rainfall regime linked to the displacements of the SPCZ. Nevertheless the above-cited authors did not entirely rule out the influence of advective processes by current anomalies.

Since the early analysis of *Delcroix and Hénin* [1989], the VOS program has been maintained, and was improved in 1992 when vessels were equipped with thermosalinographs (TSG) [*Hénin and Grelet*, 1996]. Currently, we possess 25 years (1976-2000) of SSS and SST measurements in the SWTP region, encompassing 6 El Niño and 3 La Niña events. The aim of this study is to describe the seasonal and interannual variability of SSS and SST in the SWTP and in particular the above-mentioned frontal region. In addition, some tentative explanations accounting for the observed patterns are investigated using satellite-derived precipitation data and surface geostrophic current anomalies computed from altimeter measurements.

The paper is structured as follows. SSS, SST, precipitation data, and their processing and gridding procedure are shown in section 2. Mean field and seasonal cycles of SSS, SST, and precipitation are briefly described in section 3 to put our analysis in context. The ENSO variability of the above parameters is then examined in section 4 using an Empirical Orthogonal Function (EOF) analysis. A conclusion appears in section 5.

2. Data and data processing

2.1. SSS and SST measurements

In-situ SSS and SST measurements, collected through a VOS program initiated by IRD (Institut de Recherche pour le Développement, formerly ORSTOM) in 1969 constitute the main source of data for this study. Before 1992, meteorological buckets were employed to collect salinity samples and measure SST along regular shipping routes. Bucket measurements were generally made every 30-

60 nautical miles (50-100 km) at about every 6 hours. From 1992, these merchant ships were equipped with ThermoSalinoGraphs (TSG) [*Hénin and Grelet*, 1996] which provide one measurement every 15 seconds. Before being entered in the data base, a median filter is applied to TSG time series to give one value every 5 minutes. In the present analysis a median filter was applied to the 5-minutes time series to give one value representing one hour-measurements.

Hénin and Grelet [1996] deduced the quality of the bucket and TSG measurements through comparison with simultaneous Conductivity-Temperature-Depth (CTD) measurements. Bucket data are less accurate than TSG data, and the 'bucket minus CTD' difference is much more variable than the 'TSG minus CTD' difference. Taking CTD data as a reference, we added the following values obtained by *Hénin and Grelet* [1996] to the measurements: bucket salinity (-0.1), bucket temperature (-0.15), TSG salinity (+0.02), and TSG temperature (-0.2).

About 115 000 SSS and SST (41% bucket, 59% TSG, 0.02% CTD) observations were collected in the study area. Before being entered in the data base, the following validation tests were applied to the bucket and TSG measurements: a) for each voyage, data were plotted on a map to detect position errors, and obvious outliers b) within the tropics, SSS lower than 30 or greater than 37 were rejected. TSG data were also visually compared to mean monthly values ±1 standard deviation. For the purpose of the present study, an additional validation test was then applied. Data were grouped in 2° latitude by 10° longitude bins. In a given bin, individual measurements greater/lower than the climatological monthly value plus or minus 5, 4, and 3.5 times the standard deviation were rejected. At the end of the additional test, 1% of the SSS and 2% of the SST data were rejected.

The data were then averaged on a monthly basis and gridded (2° latitude x 10° longitude x 1 month) using a triangle-based linear interpolation. The number of SSS data per month in the area under study is displayed in Figure 2. The SST data distribution presents almost the same pattern (not shown). Between 200 and 400 measurements were taken per month before 1992 when the VOS were equipped with TSGs. After that date there is a significant increase up to 1200/month. The mean number of measurements per month in every bin is shown in Figure 3. There are fewer than 5 measurements per month in the center of the region, and east of 170°E, south of 22°S and north of 14°S. It must be noted that this spatial distribution reflects a difference in temporal distribution. While

time series are almost complete in the center of the region, there are practically no data after 1992 east of 180°W, south of 22°S and north 13°S, making any extrapolation dubious. Therefore the bins east of 180°W, south of 22°S and north 13°S were excluded from the analysis.

2.2 Additional data

Rainfall data are derived from the analysis of *Xie and Arkin* [1997]. They result from the merging of different data sources: rain gauges, a number of satellite estimates, and forecasts from the NCEP (National Centers for Environmental Prediction) re-analysis. The data are available monthly, on a 2.5°-latitude by 2.5°-longitude spatial grid, from 1979 to 2000. To match the SST-SSS grid size, we first interpolated the rainfall data every 2° of latitude, and then averaged the data over 10° of longitude.

Two sets of data relative to satellite-derived surface current anomalies are available: GEOSAT from November 1986 to February 1989 [*Picaut et al.*, 1990; *Delcroix et al.*, 1994], and TOPEX/Poseidon from October 1992 to October 2000 [*Delcroix et al.*, 2000]. Anomalies of zonal and meridional geostrophic velocity are computed every 5 days on a 0.5°-latitude by 5°-longitude grid. For GEOSAT, the anomalies are computed relatively to the 1986-1989 period, while the TOPEX/Poseidon anomalies are computed relatively to the 1993-1995 period. Comparison of velocity anomalies deduced from the TOPEX/Poseidon altimeter data with the current anomalies given by Doppler current measurements made at the equator with the Tropical Atmosphere-Ocean (TAO) array gave good results [*Delcroix et al.*, 1994; *Delcroix et al.*, 2000]. Given the absence of direct current measurements away from the equator, this type of comparison cannot be made in the SWTP. As geostrophic computation is directly related to the inverse of the Coriolis parameter, computation errors decrease away from the equator. We are thus reasonably confident about the anomalies of geostrophic velocities computed in the SWTP.

The *da Silva et al* [1994] data base derived from the Comprehensive Ocean-Atmosphere Data Set (COADS) includes one of the longest available evaporation time series. It was computed using bulk formulas and ship report data. In *da Silva et al*'s atlas, this parameter is available on a monthly

basis from 1976 to 1993, on a 1°x1° horizontal grid. The data were averaged over a spatial 2°x10° grid.

Finally, surface wind stress τ will be used to evaluate the magnitude of the Ekman drift ($u_e = \tau_y/\rho fh$; $v_e = -\tau_x/\rho fh$; where f is the Coriolis parameter, ρ the sea-water density, and h the depth of the Ekman layer). In this study we computed the surface wind stress from the Florida State University (FSU) pseudo-windstress [*Legler and O'Brien,* 1988] available on a monthly basis, on a 2° latitude by 2° longitude grid. Data were averaged over 10° of longitude to fit the SSS and SST grid size.

3. Mean fields and seasonal variability

3.1 Mean fields

Mean SST and SSS distributions over the Pacific Ocean, from 1979 to 1992, are summarized in *Delcroix* [1998]; figure 2 of this paper being reproduced here (Figure 1). A zoom on the SWTP region is presented in Figure 4 for the 1976-2000 period. These maps are very similar to those presented in *Delcroix and Hénin* [1989], computed for the years 1979-81+1984-85, but excluding the 1982-1983 El Niño period.

This region is characterized by a horizontal SSS gradient between the south-eastward oriented tongue of fresh water featuring the warm pool in the north-west part of the study area, and the westward oriented tongue of high salinity water advected by the southern branch of the South Equatorial Current from the central south Pacific (Figure 4a). The low-salinity tongue lies under the SPCZ, and minimum salinity (< 34.7) is found where precipitation is maximum at 10°S-175°E (>0.25 m/month) (Figure 4c). Precipitation is low on either side of the SPCZ, in the southwest corner close to New Caledonia, and in the east, in French Polynesia, where salinity is highest.

The SST field presents quasi-zonally oriented isotherms, with waters warmer than 28°C north of 16°S. The 28°C isotherm is generally used as an arbitrary limit defining the area of the warm pool. South of 16°S the meridional gradient of SST increases, and SST falls below 25°C south of 22°S.

Seasonal and interannual variability is apparent in the monthly time series of SSS averaged over the SWTP region (figure 5). During non-ENSO years (for example during the 1979-1982 or

1984-1986 periods), SSS is minimum in March (around 35.1) and maximum in September (around 35.4). The interannual variability of SSS is clearly linked to El Niño or La Niña, as a significant divergence from the mean (35.29) is observed following extreme values of the SOI curve. SSS increases during El Niño (1976/77, 1982/83, 1987, 1991/92, 1993, 1997/98) and decreases during La Niña (1988/89, 1986, 1998/99/00). The greatest divergences occurred during the 1982/83 El Niño, when SSS reached 35.85, and during the 1988/99/00 La Niñas, when SSS decreased to 34.75.

In order to quantify the relative amplitude of the seasonal and interannual signals and to obtain a synthetic view of seasonal and inter-annual variability, an EOF analysis is performed on SSS, SST, and rainfall fields. For each parameter, the "high frequency" signal is separated from the interannual one in the following manner: we first smooth the original time series with a 25-month Hanning filter [*Blackman and Tuckey*, 1958] to get variations at periods >12 months, then subtract the original time-series from the filtered ones to obtain variations at periods ≤12 months. The EOF analysis is applied separately to each variable: on the "high frequency" variations to focus on seasonal oscillations, and on the "low frequency" variations to focus on the ENSO-like oscillations. In this procedure, the twelve-first and twelve-last months of the time series cannot be filtered, and are therefore excluded from the analysis. In the following section we describe the EOF performed on the "high frequency" variations.

3.2 Seasonal variability

The first EOF on SSS represents 31% of the data variance (12% for EOF 2). A seasonal cycle is apparent in the SSS time function (Figure 6a), with low salinities around March and high salinities around September. Maximum salinity variability has a diagonally oriented shape from Samoa (~14°S-172°W) to French Polynesia (~16°S-145°W), roughly along the mean axis of the SPCZ (Figure 6b). The amplitude of the seasonal signal, from maximum to minimum, is about 0.5 in the Samoa region (peak to peak variation of about 2x0.25). This amplitude is minimum in the south close to New Caledonia (peak to peak variation of 0.1).

The first EOF on SST represents 81% of the data variance (3% for EOF 2). The time function variability is clearly dominated by seasonal fluctuations (Figure 7a). As expected, high (low)

temperatures are found during the austral summer (winter). The spatial pattern presents zonally-oriented isolines reflecting low amplitude variations in the north-east corner of the study area (~1°C, from peak to peak), and high amplitude variations in the south-west, close to New Caledonia (>2.5°C) (Figure 7b).

The first EOF on rainfall, which represents 51% of the variance (18% for EOF 2), reflects seasonal variations, with maximum (minimum) precipitation during the austral summer (winter) (Figure 8a). The maximum amplitude of variation (~0.25 m/month from peak to peak) is situated around 13°S-170°W, close to maximum SSS variation (Figure 8b and figure 6b). Seasonal variability diminishes gradually southward to about ~0.06 m/month (from peak to peak).

The second EOF of these parameters are not discussed here as we found no obvious related physical mechanisms.

4. Interannual variability

4.1 EOF Analysis

As shown in the previous section, SSS, SST, and rainfall are influenced by seasonal variability, but modulation at longer periods is clearly visible in the original time series (Figure 5). We now present the "low frequency" time series and compare them to the SOI, smoothed with a 25-month Hanning filter.

4.1.a Sea surface salinity

The first EOF on SSS represents 58% of the data variance. The time function (Figure 6c) is well correlated with the SOI (R_0=0.70 with no time lag, R_{max}=0.73 with a two-month time lag). The spatial pattern (Figure 6d) indicates that maximum variability is centered near 15°S-175°W along the mean axis of the SPCZ. It should be noted that the 'seasonal' and ENSO-related signals display very similar spatial patterns (Figure 6b and 6d), indicating the key role of the SPCZ. During El Niño events (1976/77, 1982/83, 1986/87, 1991/92, 1993, 1997/98), the SWTP is saltier than during La Niña events (1988/89, 1996, 1998/99/00). In early 1983, during the 1982/83 El Niño, the increase in salinity was 0.5, in the Samoa-Fiji region. In 1989, during the 1988/89 La Niña event, the decrease in salinity was

0.62 in the same region. Thus in the SWTP, ENSO signals have twice the impact of seasonal signals on SSS.

The agreement between the SOI and SSS is less convincing during the 1993-1995 period (Figure 6c). While the SOI stayed negative from 1992 to the end of 1995, SSS returned to mean values around mid-1993 and was fresher than average from the beginning of 1994 to mid-1996, rather as if the SWTP were not influenced by the quasi-permanent unusual El Niño conditions that lasted from 1993 to 1995 at the equator [*Trenberth and Hoar*, 1996; *Latif et al.*, 1997]. The strong 1997/98 El Niño event gave rise to the smallest positive SSS anomaly of the observed El Niños in the time series, and the greatest negative anomalies of the period of study were observed during the 1998/99 La Niña event. Due to the filtering technique, the 1999/00 La Niña does not appear on figure 6c, but the monthly time series of SSS averaged over the SWTP region indicates that the negative SSS anomaly in 2000 is as great as in 1999 (Figure 5).

No clear explanation was found to account for the second EOF which retains 19% of the total variance.

4.1.b Sea surface temperature

The first EOF on SST represents 45% of the variance (21% for EOF 2). Correlation between the time function and the filtered SOI curve is R_0=0.51 with no lag, and R_{max}=0.53 with a 2-month lag (Figure 7c). SST is colder (respectively warmer) during El Niño (respectively La Niña) events, which is consistent with *Delcroix and Lenormand*'s [1997] analysis for the New Caledonia sector (22°S-165°E). The amplitude of variation due to inter-annual variability (~0.75°C maximum in 1996 and 1999, in the Vanuatu region) is less pronounced than the amplitude of the seasonal variations. Though weak, this ENSO signal is still detectable in the paleorecord of coral drilled in Vanuatu [*Corrège et al.*, 2000]. Maximum interannual variability occurred at the southern edge of the mean position of the warm pool, in between Vanuatu and the Fiji islands (Figure 7d). In spite of a good phasing agreement (Figure 7c), there is no obvious link between the intensity of the SOI and the amplitude of the SST anomaly. Indeed, the very strong 1982/83 El Niño event has a much weaker SST signature than the

smaller 1986/87 event. The greatest anomalies occurred during the 1996 La Niña, although the SOI is only slightly positive, and during the 1999/00 La Niña.

4.1.c Precipitation

The first EOF on precipitation represents 53% of the variance (19% for the EOF 2). There is a clear correlation between the time function and the SOI (R_0=0.80 with no lag, R_{max}=0.87 with 2- and 3-month lag) (Figure 8c). The spatial pattern (Figure 8d) indicates that rainfall interannual variability has a converse signal on the southwestern and the northeastern sides of the SWTP. There is a precipitation shortage (excess) over Samoa, Fiji, Vanuatu, Solomon, and New Caledonia during El Niño (La Niña) events, while there is a slight precipitation excess (shortage) over French Polynesia. This pattern is in line with the global analysis made by *Meehl* [1987] indicating that during strong monsoon events over India, corresponding roughly to La Niña events, rainfall increased to the west of the SPCZ axis, and decreased to the east of the SPCZ axis. This is also in agreement with regional analysis made for New Caledonia from a set of rain gauge stations [*Morlière and Rebert*, 1986; *Nicet and Delcroix*, 2000], and for Samoa/Wallis [*Alory and Delcroix*, 1999]. The amplitude of variation due to low frequency modulation is less pronounced than that of seasonal variation. For example, the precipitation shortage due to the 1982/83 El Niño in Fiji (18°S-178°W) is about -0.04 m/month, and the precipitation excess during the 1988/89 La Niña event in the same region is 0.06 m/month. This can be contrasted with the amplitude (from minimum to maximum) of the seasonal signal which is of the order of 0.2 m/month. In New Caledonia (22°S-165°E), where seasonal variations are amongst the lowest in the SWTP (Figure 8b), and interannual variability is high (Figure 8d), *Nicet and Delcroix* [2000] showed that ENSO-related precipitation changes range within 20%-50% of the mean annual values.

4.1d Evaporation

In order to test the potential effect of evaporation changes on SSS variability, we used the *da Silva et al.* [1994] data covering the 1976-1993 period. The 1976-1993 averaged evaporation values (not shown) are minimum below the mean SPCZ axis (~0.13 m/month) and maximum south of it, between Fiji and New Caledonia (~0.15 m/month). The first EOF (not shown) extracts a clear seasonal

signal in the SWTP, with maximum variability south of 16°S and minimum variability along 10°S. The amplitude (from maximum to minimum) of the seasonal variation is about 0.08 m/month, weaker than the seasonal precipitation cycle. This means that the seasonal variation in the 'Precipitation minus Evaporation' difference is mainly dependent on precipitation. The first EOF of the low-frequency evaporation signal (not shown) is relatively flat and does not show any correlation with the SOI.

4.2 Time-space evolution of the frontal zone

4.2.a SST, SSS, and precipitation fields

Time-longitude and time-latitude plots of the SSS, SST, and precipitation fields were drawn up to further assess the relationship between changes in these parameters and ENSO. We chose to use the time-longitude plot at the latitude of 17°S (Plate 1a, 1c, 1e), where the SSS front is strongest (Figure 4a) and time series are complete for every longitude; and the time-latitude plot at the longitude of 175°E (Plate 1b, 1d, 1f), as time series are complete there from 11°S to 23°S. In these plots, data have been low-pass filtered with a 25-month Hanning filter to eliminate periods ≤12 months, and the filtered SOI is superimposed on these plots.

Plate 1a and plate 1b clearly show that the salinity front separating the low-salinity water under the SPCZ from the high-salinity waters of the south central Pacific, oscillates back and forth in the zonal/meridonal direction following the SOI. The correlation between the SOI and the displacement in longitude of the 35.5 isoline is R_0=0.59 (R_{max} equals also 0.59 with a one- and two-month lag). The correlation with the shift in latitude of the 35 isoline is R_0=0.62 (R_{max}=0.84 with a five-month lag). As the displacements occurred in both east-west and north-south directions, they indicate that the front moved in a northeast-southwest direction. Saline waters (> 35.25, shown in yellow to red in the plots) invaded the north-west portion of the area during El Niño events, at the end of 1977, 1983, 1987, 1993 and 1998; while low-salinity waters moved south-eastward during La Niña periods. Confirming the EOF analysis, the salinity front stayed close to its mean position in longitude, around 170°W, during the 1993-1995 prolonged warm events.

As the mean SST field is quasi-zonally oriented (Figure 4b), it is mainly in the north-south direction that we can observe displacements of surface isotherms. This is the case in plate 1d where

there is a tendency towards southward (respectively northward) shifts of the warm pool (SST > 28°C) during La Niña (respectively El Niño) events.

The time-evolution of the north-south movements of the precipitation field also corresponds closely to the SOI: the tongue of maximum precipitation (yellow to red in Plate 1f) extends southward (northward) during La Niña (El Niño) events, in relation to the SPCZ southwestward (northeastward) displacements. An exception occurred at the end of 1989 and the beginning of 1990 with a precipitation shortage from 11°S to 23°S, although there is no minimum in the SOI that might indicate an El Niño event (plate 1f). The time-longitude precipitation plot does not display any clear front (plate 1e). Precipitation is minimum in the east and in the west of the SWTP. In the center of the region, precipitation variability is also linked to the SOI. Precipitation is minimum in 1983, 1987,1992, and 1998, and maximum in 1981/82, 1984/85, 1989, and from 1993 to 1996.

To sum up, there are southward incursions of the warm pool in the SWTP during La Niña events. Deep atmospheric convection is closely linked to SST above 28°C, as is the position of the SPCZ (see also *Vincent* [1994]). It is thus not surprising that rainfall increases in the SWTP during La Niña events. This excess of precipitation is qualitatively consistent with interannual variation in the SSS-front position. Besides, since *Delcroix and Hénin* [1989] have shown that during the 1982/83 El Niño the South Equatorial Current was stronger than usual, zonal advection could also possibly account for the interannual displacement of the SSS front.

4.2.b Potential role of zonal and meridional advection

Reverdin et al. [1994] estimated mean surface current from buoy drifts and current meter records, between January 1987 and April 1992, for the tropical Pacific. In the SWTP, at 17°S, the mean zonal component of the surface current is westward, east of 175°E, and eastward, west of 175°E. Thus there is a tendency for zonal convergence of the surface currents to strengthen the SSS front.

One means of obtaining information on the surface currents at inter-annual time-scale is to use altimeter data, which allow computation of geostrophic current anomalies. Two major contrasting periods were sampled by the altimeters, the 1987-1989 El Niño/La Niña with GEOSAT, and the 1997-

2000 El Niño/La Niña with TOPEX/Poseidon. Anomalies of surface geostrophic zonal currents and SSS field are displayed along 17°S in plate 2 for these two periods. The velocity anomalies are generally within ±5 cms^{-1}, though they exceed these values for a few months in 1987 and in 1998-1999. During the 1987/88 El Niño, a westward anomaly (>5 cm s^{-1}) is present from February 1987 to July 1987, between 170°E and 160°W. During the second half of the 1987-year and the beginning of 1988 an eastward anomaly developed (>5 cm s^{-1}) (plate 2d). During the 1997/98 El Niño a westward velocity anomaly (>10 cm s^{-1}) occurred between 180°W and 165°W, from the beginning of 1998 to September 1998 (plate 2b). Then an eastward velocity anomaly, reaching 10 cm s^{-1}, occurred from the beginning of 1999 to July 1999. In all these cases, the westward velocity anomaly preceded by 2-3 months the westward extension of the SSS salinity tongue, and the eastward retraction of this tongue coincided with the eastward velocity anomaly (plate 2a and 2c) strongly suggesting that, qualitatively, zonal geostrophic advection plays a role in the east-west movement of the zonal front.

The meridional current anomalies computed from TOPEX/Poseidon altimeter data vary within ±2 cms^{-1} from 1992 to 1999 (not shown). A northward anomaly develops at 17°S-180°W, during the second part of 1988. This is consistent with the westward anomaly observed at the same position and the northwestward displacement of the SSS front, although this anomaly is very slight (2-3 cms^{-1}).

To obtain a complete picture, the effect of the interannual anomalies of the Ekman drift in front displacements has to be estimated. While the time function of the first EOF of the zonal component of pseudo-windstress is not correlated with the SOI, there is a very close correlation (R_{max}=0.88 with 1-month time lag) between the time function of the first EOF of the meridional component of pseudo-windstress and the SOI (not shown). This close relationship was to be expected since the SOI is a measure of the variability of the sea level atmospheric pressure gradient between Tahiti and Darwin, and so and so is tightly related to the meridional geostrophic component of the wind. It is therefore not surprising that the zonal component of the Ekman drift ($u_e = \tau_y/\rho f h$) varies in phase with the SOI: westward (eastward) anomalies of Ekman velocities occurred during El Niño (La Niña) events. One difficulty in estimating the magnitude of the Ekman velocity comes from our inability to quantitatively scale the Ekman depth (h) and its low frequency variability. Using a realistic

h=30 m at 17°S results in a westward current anomaly smaller than 3 cm s^{-1} at the beginning of 1998, and an eastward anomaly lower than 2 cm s^{-1} in January 1999 and in January 2000. These currents thus reinforce the zonal component of the geostrophic velocity although they are of a smaller order of magnitude.

Based on XBT data, *Delcroix and Hénin* [1989] showed that during the 1982/83 El Niño event isotherms rose in the northern part of the SWTP, through Ekman pumping, in relation with the northward displacement of the SPCZ. This rise was accompanied by a southward shift of the center of the large-scale anticyclonic gyre reinforcing the westward flowing SEC in the SWTP region. This southward shift during the 1982/83 El Niño event was also evident in sea level data [*Wyrtki*, 1975, 1984]. It implies a stronger than usual SEC from April to July 1983, concomitant with the northeastward displacement of the SSS front and consequently an increase of SSS in the SWTP.

5. Conclusion

The analysis of SSS, SST and precipitation changes over 25 years (1976-2000) in the SPCZ region (10°S-24°S; 160°E-140°W) brings out the close relationship between the time-variability of these parameters and El Niño or La Niña. This is consistent with previous studies limited to shorter time periods [*Delcroix and Hénin*, 1989, 1991; *Delcroix et al.*, 1996]. The present study deals with an unprecedented long time series encompassing six El Niño (1976/77, 1982/83, 1987, 1991/92, 1993, 1997/98) and three La Niña (1988/89, 1986, 1998/00) events. Our analysis confirms that SSS is higher, SST and precipitation are lower during El Niño events than during La Niña events. The amplitude of this interannual signal is an order of magnitude less than the amplitude of the seasonal signal for SST and precipitation, whereas it is twice the amplitude of the seasonal signal for SSS.

It is worth noting that the greatest anomalies of the time series (1976-2000) occurred during the last La Niña events, in 1999 and 2000 for SSS, and in 1996 and 1999 for SST. As all ENSO variations are mainly due to the southeastward (northward) displacement of the warm pool during La Niña (El Niño) events, the greatest changes in SST and SSS amplitude during the 1990s thus reflect enhanced displacements of the warm pool.

In the equatorial band, the low frequency displacements of the SSS front were shown to be mainly due to zonal advection by oceanic currents and, to a lesser extent, to the Evaporation/Precipitation budget, since the convection zone followed the migration of the warm/fresh pool [*Picaut et al.*, 1996; *Delcroix and Picaut*, 1998]. In the SPCZ region the displacement of the SSS front still correlates closely with the SOI, and it moves both zonally and meridionally along a northwest–southeast oriented axis. Surface geostrophic current anomalies reveal that in 1987/88 and 1998/99, westward and slight northward current anomalies develop for 6 months during the El Niño event, almost in phase with the north-westward displacement of the high salinity waters. These current anomalies are then reversed and give way to eastward current anomalies in phase with the south-eastward displacement of the fresh waters.

Remarkably, when the SSS front along the equator shifts eastward during an El Niño event, bringing warm and fresh waters to the central Pacific, the SSS front in the SWTP moves in the opposite direction toward the north-west, bringing salty and cold waters to the south-western tropical Pacific.

With the data available, it would be unrealistic to try to quantify the relative importance of advection versus evaporation/precipitation budget in the displacement of the SSS front. Firstly because altimetry only enables us to compute the anomalies of geostrophic currents and we do not know the mean current in the period under study. Secondly because it is difficult to obtain a reliable evaporation/precipitation budget at interannual time scale. Thirdly because we do not know the depth of the salinity mixed layer, a term which appears in the salt conservation equation. We realize that to be conclusive this analysis should be more quantitative. This could be achieved with models adequately reproducing our observations; as far as we know, this has not yet be done for the SPCZ region.

Acknowledgement.

The 1976-2000 bucket and TSG data set represents the combined effort of many IRD colleagues involved in the ship-of-opportunity program and particularly owes much to Luc Foucher, Jean-Marc Ihily, and David Varillon for the recent measurements. The satellite-derived geostrophic current anomalies were processed by François Masia, at IRD-Nouméa. We are also indebted to all our colleagues who gave us free access to their data set through the Web. We would like to thank Joël

Picaut, two anonymous reviewer, and the JGR editor and co-editor for their constructive comments on the manuscript. This work was funded by the Institut de Recherche pour le Développement (IRD) and the Programme National d'Etude de la Dynamique du Climat (PNEDC).

References

Alory, G., and T. Delcroix, Climatic variability in the vicinity of Wallis, Futuna, and Samoa islands (13°-15°S, 180°-170°W), *Oceanologica Acta, 22*, 249-263, 1999.

Blackman, R.B., and J.W. Tukey, The measurement of power spectra, *Dover Publications*, 190 pp, 1958.

Corrège, T., T. Delcroix, J. Récy, W. Beck, G. Cabioch, and F. Le Cornec, Evidence for stronger El Niño-Southern Oscillation (ENSO) events in a mid-Holocene massive coral, *Paleoceanogr., 15*, 465-470, 2000.

da Silva, A., A.C. Young, and S. Levitus, Atlas of Surface Marine Data 1994, Volume 1: Algorithms and Procedures, *NOAA Atlas NESDIS 6, U.S. Department of Commerce*, Washington, D.C., 1994.

Delcroix, T., Observed surface oceanic and atmospheric variability in the tropical Pacific at seasonal and ENSO timescales: A tentative overview, *J. Geophys. Res., 103*, 18,611-18,633, 1998.

Delcroix, T., and C. Hénin, Mechanisms of thermal structure and sea surface thermohaline variabilities in the southwestern tropical Pacific during 1975-1985, *J. Mar. Res., 47*, 777-812, 1989.

Delcroix, T., and C. Hénin, Seasonal and interannual variations of sea surface salinity in the tropical Pacific Ocean, *J. Geophys. Res., 96*, 22135-22150, 1991.

Delcroix, T., and O. Lenormand, ENSO signals in the vicinity of New Caledonia, South Western Pacific, *Oceanol. Acta, 20*, 481-491, 1997.

Delcroix, T., and J. Picaut, Zonal displacement of the western equatorial Pacific "fresh pool", *J. Geophys. Res., 103*, 1087-1098, 1998.

Delcroix, T., J.P. Boulanger, F. Masia, and C. Menkes, GEOSAT-derived sea level and surface-current anomalies in the equatorial Pacific during the 1986-1989 El Niño and La Niña, *J. Geophys. Res, 99*, 25093-25107, 1994.

Delcroix, T., C. Hénin, V. Porte, and P. Arkin, Precipitation and sea-surface salinity in the tropical Pacific Ocean, *Deep-Sea Res., 43*, 1123-1141, 1996.

Delcroix, T., B. Dewitte, Y. du Penhoat, F. Masia, and J. Picaut, Equatorial waves and warm pool displacements during the 1992-1998 El Niño Southern Oscillation events: observation and modeling, *J. Geophys. Res., 105*, 26045-25062, 2000.

Hénin, C., and J. Grelet, A merchant ship thermo-salinograph network in the Pacific Ocean, *Deep-Sea Res. I, 43*, 1833-1855, 1996.

Latif, M., R. Kleeman, C. Eckert, Greenhouse warming, decadal variability, or El Niño? An attempt to understand the anomalous 1990s, *J. Climate*, 10, 2221-2239, 1997.

Legler, D.M., and J.J. O'Brien, Tropical Pacific wind stress analysis for TOGA, in *IOC Time Series of Ocean Measurements, IOC Tech. Ser., vol. 4*, UNESCO, Paris, 1988.

Meehl, G.A., The annual cycle and interannual variability in the tropical Pacific and Indian Ocean regions, *Mon. Wea. Rev., 115*, 27-50, 1987.

Morlière, A., and J.P. Rebert, Rainfall Shortage and El Niño-Southern oscillation in New Caledonia, southwestern Pacific, *Mon. Wea. Rev., 114*, 1131-1137, 1986.

Nicet, J.B., and T. Delcroix, ENSO-Related precipitation changes in New Caledonia, southwestern tropical Pacific: 1969-98, *Mon. Wea. Rev., 128*, 3001-3006, 2000.

Pazan, S.E., and G. Meyers, Interannual fluctuations of the tropical Pacific wind field and the Southern Oscillation, *Mon. Wea. Rev., 110*, 587-600, 1982.

Picaut, J., A. Busalacchi, M.J. McPhaden, and B. Camusat, Validation of the geostrophic method for estimating zonal currents at the equator from Geosat altimeter data, *J. Geophys. Res., 95*, 3015-3024, 1990.

Picaut, J., M. Ioualalen, C. Menkes, T. Delcroix, M.J. McPhaden, Mechanism of the zonal displacements of the Pacific warm pool: Implications for ENSO, *Science, 274*, 1486-1489, 1996.

Picaut, J., F. Masia, and Y. du Penhoat, An advective-reflective conceptual model for the oscillatory nature of ENSO, *Science, 277*, 663-666, 1997.

Picaut, J., M. Ioualalen, T. Delcroix, F. Masia, R. Murtugudde, and J. Vialard, The oceanic zone of convergence on the eastern edge of the Pacific warm pool: A synthesis of results and

implications for El Niño-Southern Oscillation and biogeochimical phenomena, *J. Geophys. Res., 106*, 2263-2386, 2001.

Reverdin, G., C. Frankignoul, E. Kestenare, and M.J. McPhaden, Seasonal variability in the surface currents of the equatorial Pacific, *J. Geophys. Res., 99*, 20323-20344, 1994.

Trenberth, K.E., and T.J. Hoar, The 1990-1995 El Niño-southern oscillation event: longest on record, *Geophys. Res. Letters, 23*, 57-60, 1996.

Vialard, J., and P. Delecluse, An OGCM study for the TOGA Decade. Part II: Barrier-Layer Formation and Variability, *J. Phys. Oceanogr., 28*, 1089-1106, 1998.

Vincent, D.G., The south pacific convergence zone (SPCZ): a review, *Mon. Wea. Rev., 122*, 1949-1970, 1994.

Wyrtki, K., Fluctuations of the dynamic topography in the Pacific Ocean, *J. Phys. Oceanogr., 5*, 450-459, 1975.

Wyrtki, K., A southward displacement of the subtropical gyre in the south Pacific during the 1982-1983 El Niño, *Tropical ocean-atmosphere Newsletter, 23*, 14-15, 1984.

Xie, P., and P.Arkin, Global precipitation: a 17-year monthly analysis based on gauge observations, satellite estimates, and numerical model outputs, *Bull. Amer. Meteor. Soc., 78*, 2539-2558, 1997.

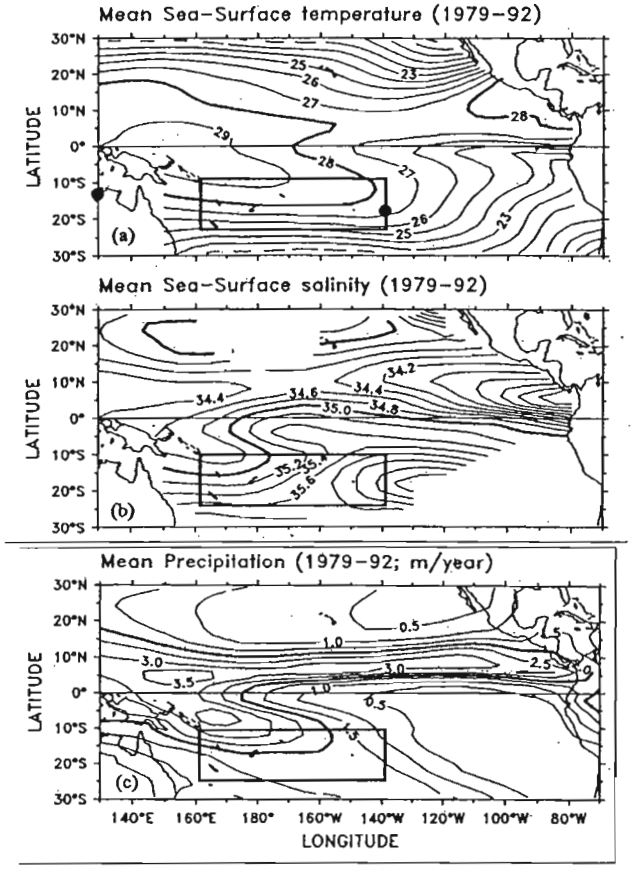

Figure 1. Mean (a) sea surface temperature (in °C), (b) sea surface salinity, and (c) precipitation (m/year), averaged over 1979-1992 [*from Delcroix*, 1998]. The South Western Tropical Pacific zone (24°S-10°S/160°E-140°W) is indicated by the rectangle. The black dots in (a) denote Darwin (Australia) and Tahiti (French Polynesia).

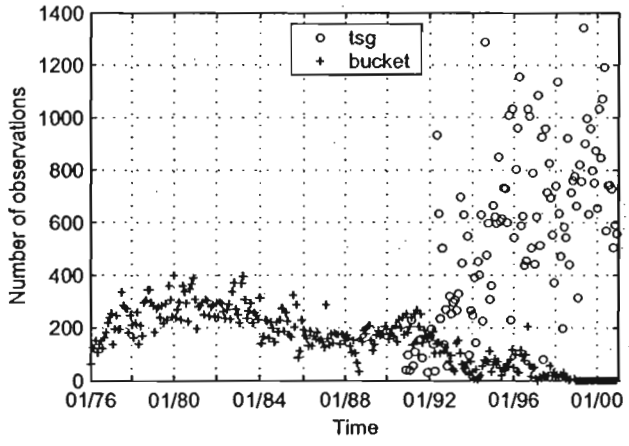

Figure 2. Monthly-number of bucket (crosses) and thermosalinograph (circles) measurements of sea surface salinity in the South Western Tropical Pacific, from 1976 to 2000.

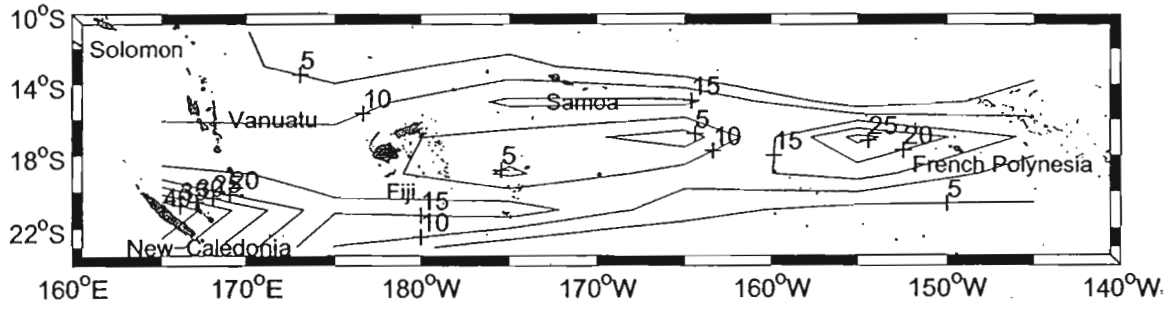

Figure 3. Mean monthly number of sea surface salinity measurements in the South Western Tropical Pacific, in 2°-Latitude by 10°-Longitude cells, from 1976 to 2000.

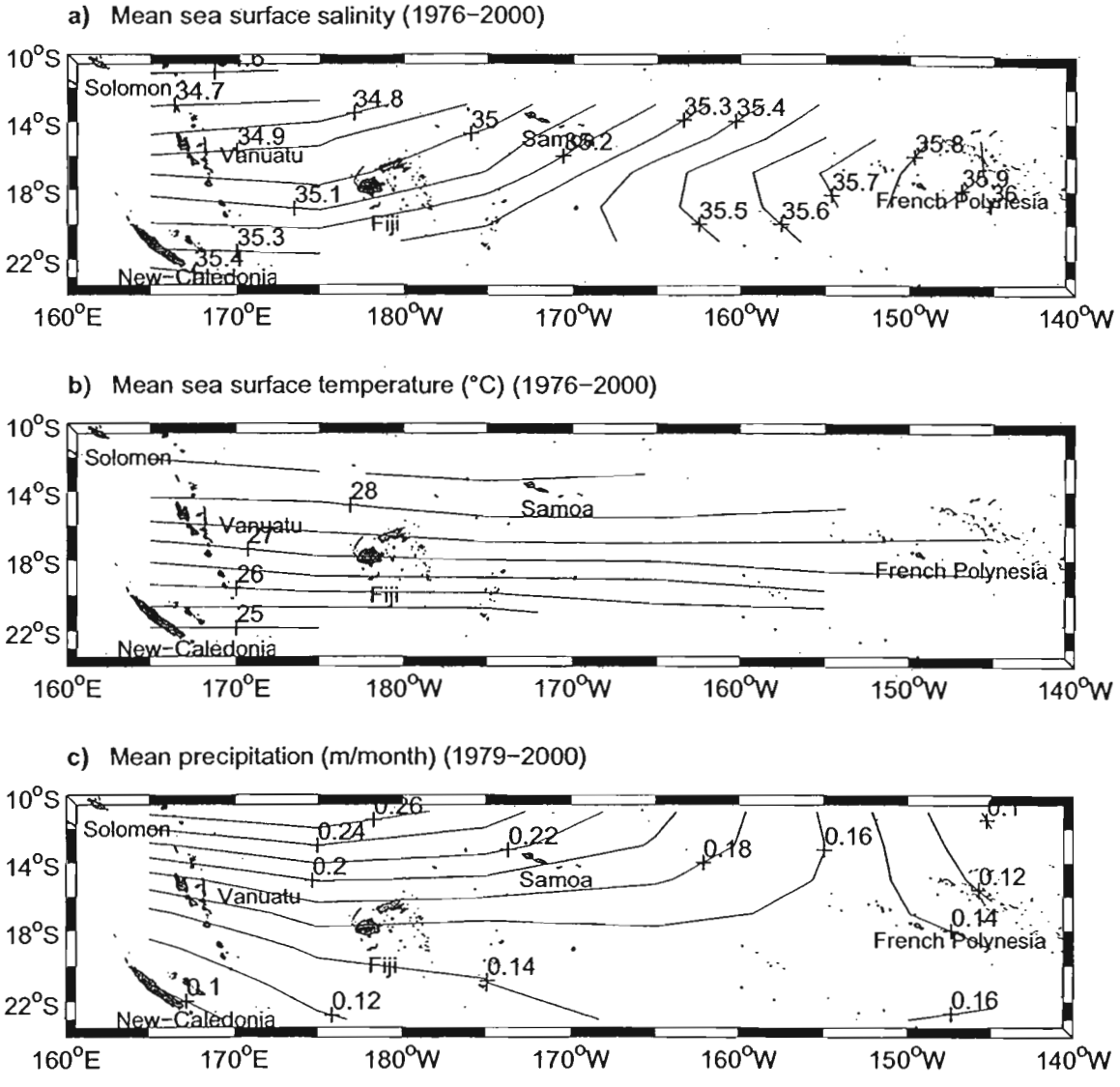

Figure 4. Mean (a) sea surface salinity, (b) sea surface temperature in °C, (c) precipitation in m/month. Precipitation is averaged between 1979 and 2000, the other fields are averaged between 1976 and 2000.

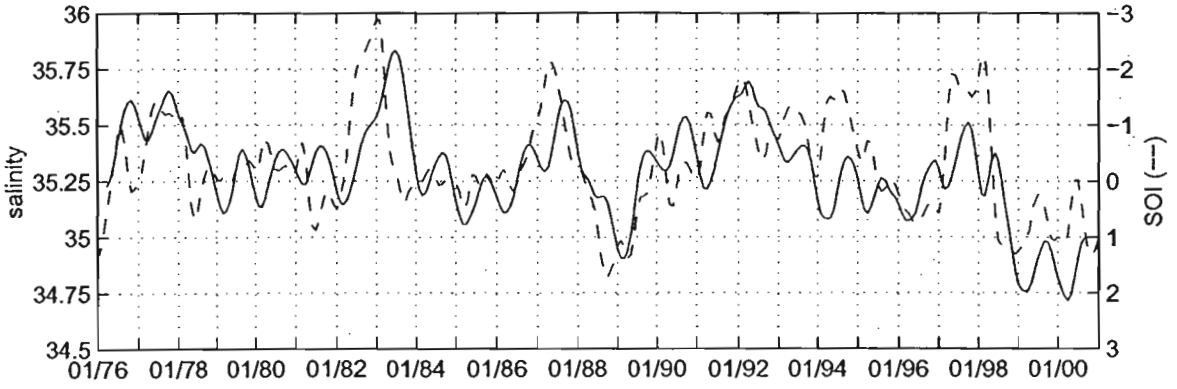

Figure 5. Monthly time series of sea surface salinity (solid line) averaged in the South Western Tropical Pacific and SOI curve (dashed line). Both time series are low-pass filtered with a 3-month Hanning filter. Note that the SOI axes is reversed.

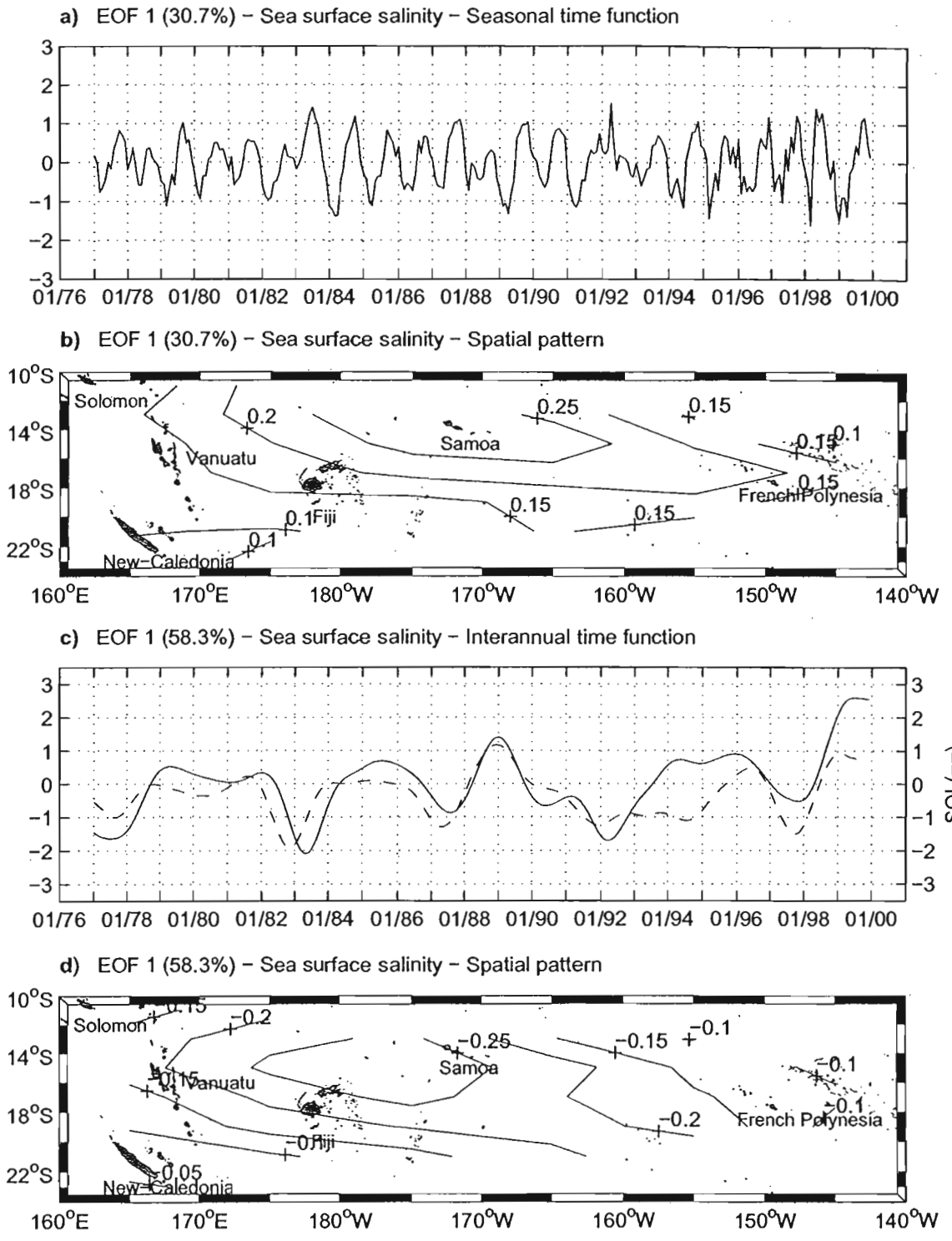

Figure 6. First mode of the empirical orthogonal function in sea surface salinity in the South Western Tropical Pacific.

(a) time function and (b) spatial pattern of the 'seasonal' time series. The 'seasonal' time series is defined as the difference between the monthly time series minus the 25-month filtered time series.

(c) time function (solid line) and (d) spatial pattern of the 'interannual' time series. The 'interannual' time series is computed by filtering the monthly time series with a 25-month Hanning filter. Superimposed on the time function is the 25-month filtered SOI (dashed line). The units are so defined that the product between the spatial pattern and the time function denotes PSU.

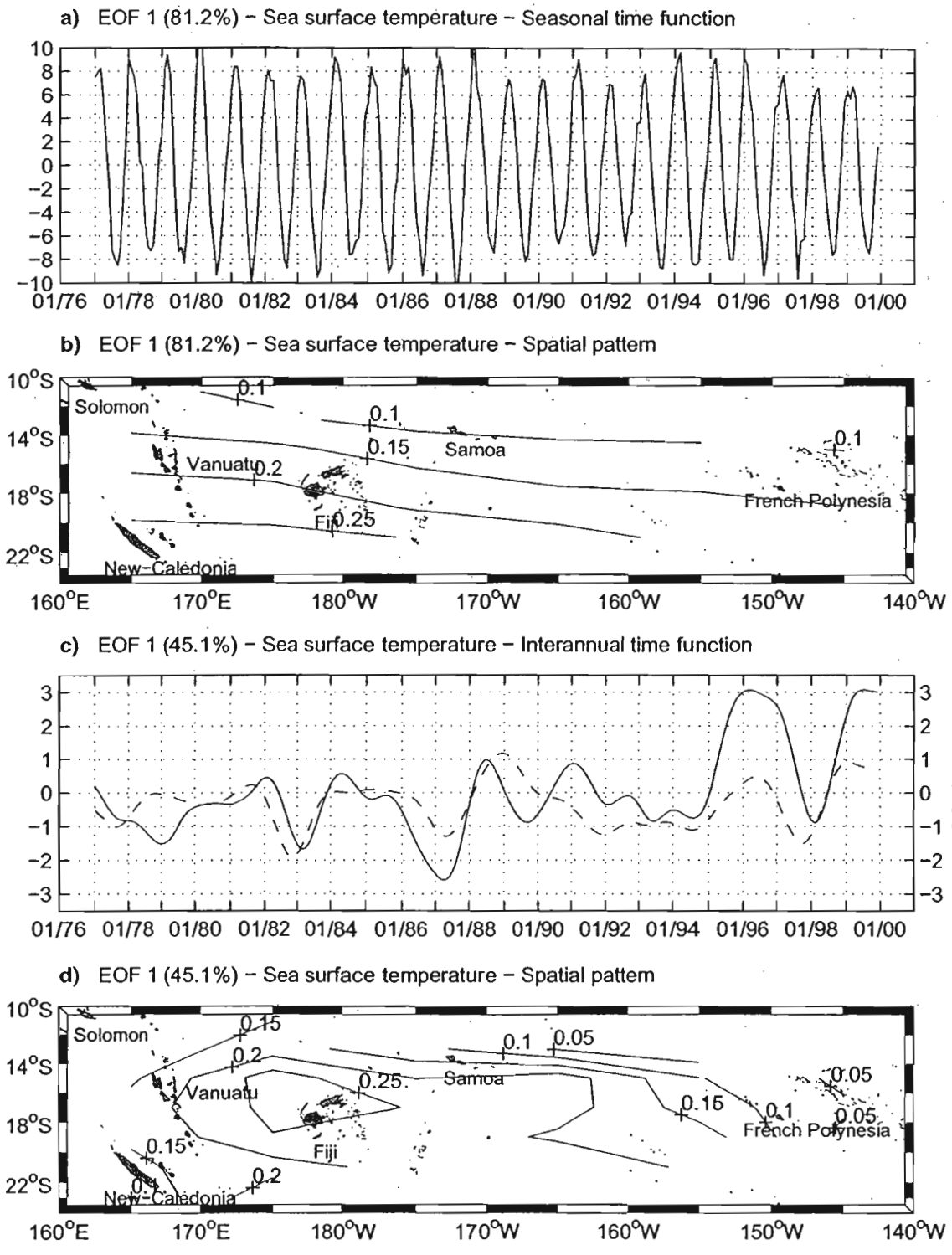

Figure 7. Same as Figure 6 for the sea surface temperature. The units are so defined that the product between the spatial pattern and the time function denotes °C.

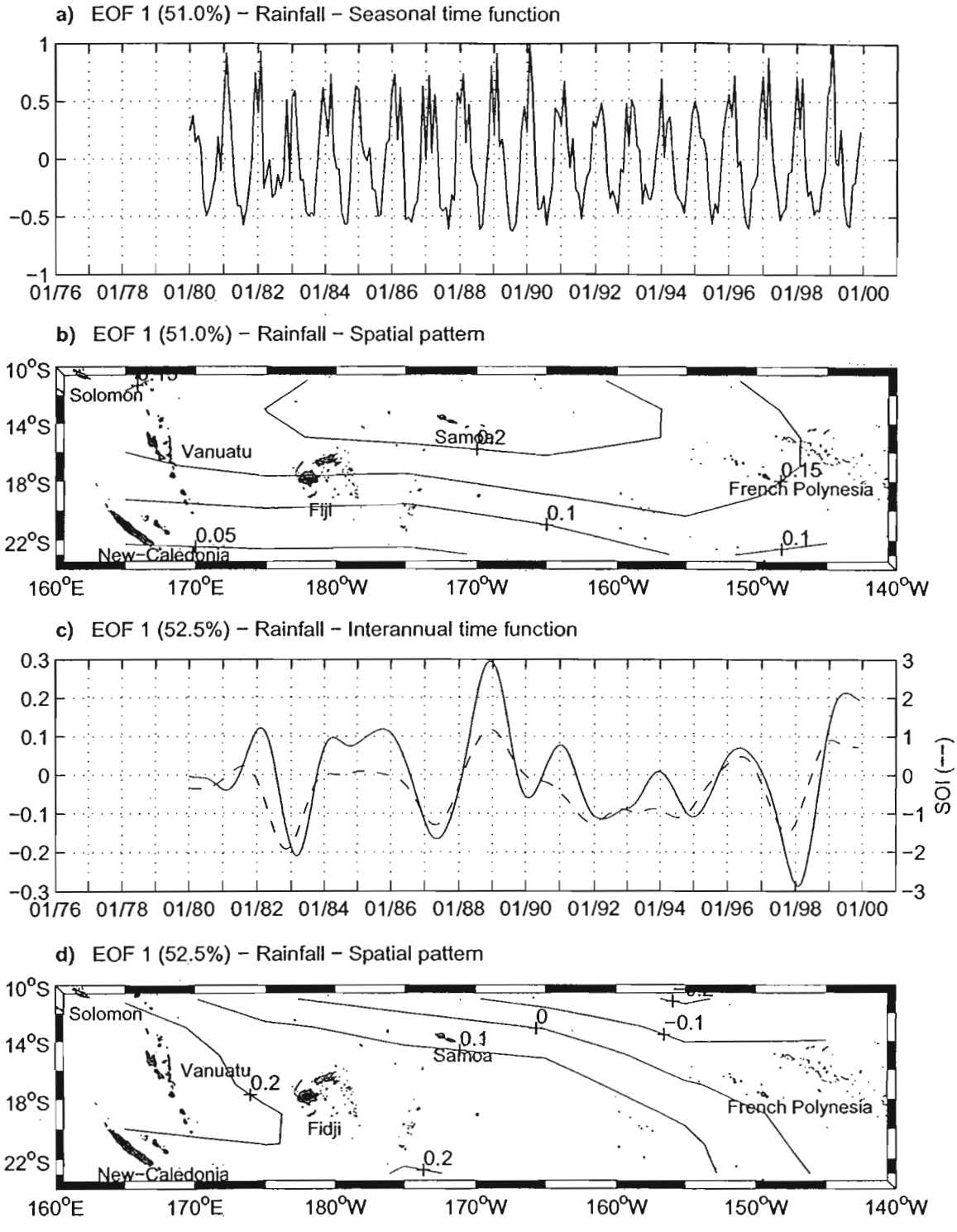

Figure 8. Same as Figure 6 for the precipitation. The units are so defined that the product between the spatial pattern and the time function denotes m/month.

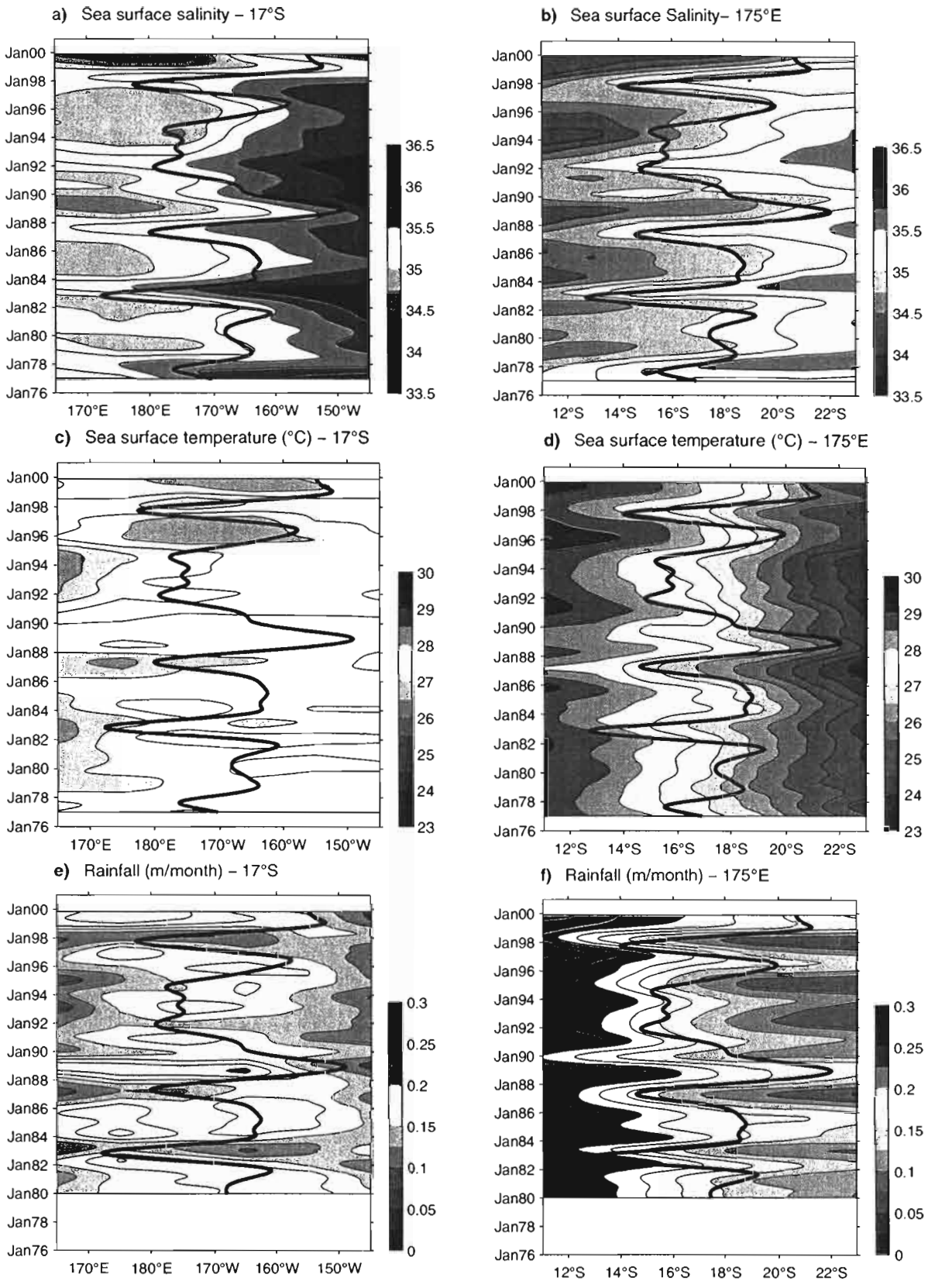

Plate 1. Time-longitude plots along 17°S, of the (a) sea surface salinity, (c) sea surface temperature in °C, and (e) precipitation in m/month.
Time-latitude plots along 175°E of the (b) sea surface salinity, (d) sea surface temperature in °C, and (f) rainfall in m/month. Time series has been low-pass filtered with a 25-month Hanning filter.
Superimposed on every diagram is the 25-month filtered SOI. Negative (positive) values of the SOI are towards the left (right) of every figure. The scale of the SOI on the x-axis is comprised between 1.5 and -2.5 with the zero close to the 165°W longitude for plots a, c, e, and close to the 18.5°S latitude for plots b, d, f.

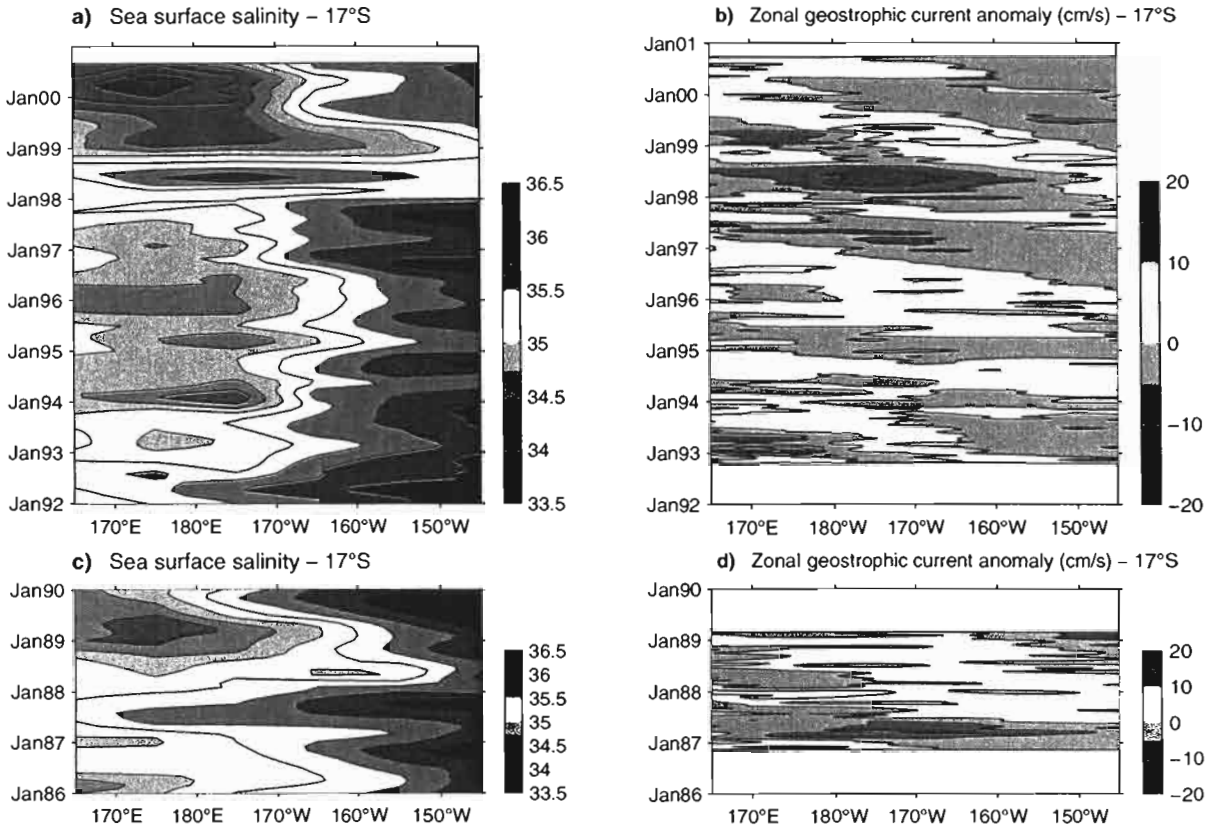

Plate 2. Time-longitude plots along 17°S, of the (a) 3-month Hanning filtered sea surface salinity between 1992 and 2000, (b) anomaly, referring to the period 1993-1995, of the zonal component of surface geostrophic current (in cms^{-1}) computed from TOPEX/Poseidon altimeter data, (c) 3-month Hanning filtered sea surface salinity between 1986 and 1989, (d) anomaly, referring to the period 1986-1989, of the zonal component of surface geostrophic current (in cms^{-1}) computed from GEOSAT altimeter data.

PALEOCEANOGRAPHY, VOL. 15, NO. 4, PAGES 465-470, AUGUST 2000

Evidence for stronger El Niño-Southern Oscillation (ENSO) events in a mid-Holocene massive coral

Thierry Corrège,[1] Thierry Delcroix,[1] Jacques Récy,[1] Warren Beck,[2] Guy Cabioch,[1] and Florence Le Cornec[3]

Abstract. We present a 47-year-long record of sea surface temperature (SST) derived from Sr/Ca and U/Ca analysis of a massive *Porites* coral which grew at ~ 4150 calendar years before present (B.P.) in Vanuatu (southwest tropical Pacific Ocean). Mean SST is similar in both the modern instrumental record and paleorecord, and both exhibit El Niño-Southern Oscillation (ENSO) frequency SST oscillations. However, several strong decadal-frequency cooling events and a marked modulation of the seasonal SST cycle, with power at both ENSO and decadal frequencies, are observed in the paleorecord, which are unprecedented in the modern record.

1. Introduction

In the last two decades we have witnessed a change in the mode of El Niño-Southern Oscillation (ENSO), with more frequent and stronger El Niño events [*Trenberth and Hoar*, 1996, 1997; *Trenberth and Hurrell*, 1994]. Whether this modulation of ENSO is a result of superimposition of other natural oceanic cycles or is induced by some external factor, such as increasing atmospheric greenhouse gases, is still debated [*Harrison and Larkin*, 1997; *Holbrook and Bindoff*, 1997; *Latif et al.*, 1997; *Guilderson and Schrag*, 1998; *Zhang et al.*, 1998] and is a question of some importance to predictive models of climate change. One way to differentiate among the potential causal agents is to examine ENSO behavior from a time period where increasing greenhouse gasses is not an issue. Since instrumental sea surface temperature (SST) records do not extend that far back in time, we have to rely on proxies to generate long, high-resolution SST data sets. It is now well established that some trace elements (Sr and U, in particular) incorporated in the aragonitic skeleton of scleractinian corals provide a robust paleothermometer [*Beck et al.*, 1992; *Min et al.*, 1995; *Alibert and McCulloch*, 1997]. In a previous contribution [*Beck et al.*, 1997] we presented the progressive warming of the tropical southwest Pacific during the deglaciation based on analyses of corals drilled on Espiritu Santo, Vanuatu (15°40'S; 167°00'E). A 5-year section of an otherwise 47-year-long *Porites* colony revealed a large year-long cooling event dated at 4166±15 calendar years B.P. (U/Th date performed by W. Beck in the Department of Geology and Geophysics, University of Minnesota), which remained unexplained [*Beck et al.*, 1997]. This cold snap prompted us to analyze the entire colony in order to investigate whether this was a recurrent feature, and if so, whether strong ENSO events could be invoked as a possible cause for the cooling. In the present contribution we first look at the modern instrumental SST record from Vanuatu in order to characterize the ENSO signal in this area and then compare the modern SST and paleo-SST records.

2. Material and Method

We first collected a live *Porites* coral from Amédée Lighthouse, near Nouméa (New Caledonia) in 1992. The coral was slabbed, X-rayed, and cleaned in an ultrasonic bath prior to sampling. On average, 12 samples per year were taken continuously along the main growth axis using a dental burr and a three-axis positioning system. The aragonitic powder was then dissolved in 2% spiked nitric acid, and Ca, Sr, and U were analyzed with a Varian Ultramass inductively coupled plasma mass spectrometer (ICP-MS) following a new technique [*Le Cornec and Corrège*, 1997]. A coral sample from New Caledonia (labeled NC20) was reduced to powder, sieved with a 40-μm mesh, and used as a standard. Replicate analyses of NC20 yield an external reproducibility (2σ) of 0.05 mmol/mol for Sr/Ca (~0.7°C) and of 0.01 μmol/mol for U/Ca (~0.3°C). Sr/Ca and U/Ca analyses were fitted to the instrumental SST record from Amédée Lighthouse for the 1981-1990 period (Figures 1 and 2) using the Analyseries program [*Paillard et al.*, 1996]. Each tracer was then regressed against SST, and the regression yielded the following equations:

$$\mathrm{Sr/Ca}\ (10^{-3}\ M) = 10.73 - 0.0657\mathrm{SST} \quad R = 0.79,$$

$$\mathrm{U/Ca}\ (10^{-6}\ M) = 2.106 - 0.0367\mathrm{SST} \quad R = 0.89.$$

The precision (standard error of estimate) [*Runyon et al.*, 1996; *Bevington and Robinson*, 1992] calculated from these equation is ±1.3°C for the Sr/Ca thermometer and ±0.9°C for the U/Ca thermometer. This is slightly higher than the precision of the Sr/Ca thermometer using thermal ionization mass spectrometry which has been estimated to be ±0.3°C [*Alibert and McCulloch*, 1997].

The same procedures were used for the sampling and analyses of the fossil coral from Tasmaloum (Vanuatu). This coral was found between 0.80 and 1.20 m depth in drill core 9A,

[1] Institut de Recherche pour le Développement, Nouméa, New Caledonia.
[2] National Science Foundation Arizona Accelerator Mass Spectrometry Facility, Department of Physics, University of Arizona, Tucson.
[3] Laboratoire des Formations Superficielles, Institut de Recherche pour le Développement, Bondy, France.

Paper number 1999PA000409.
0883-8305/00/1999PA000409$12.00

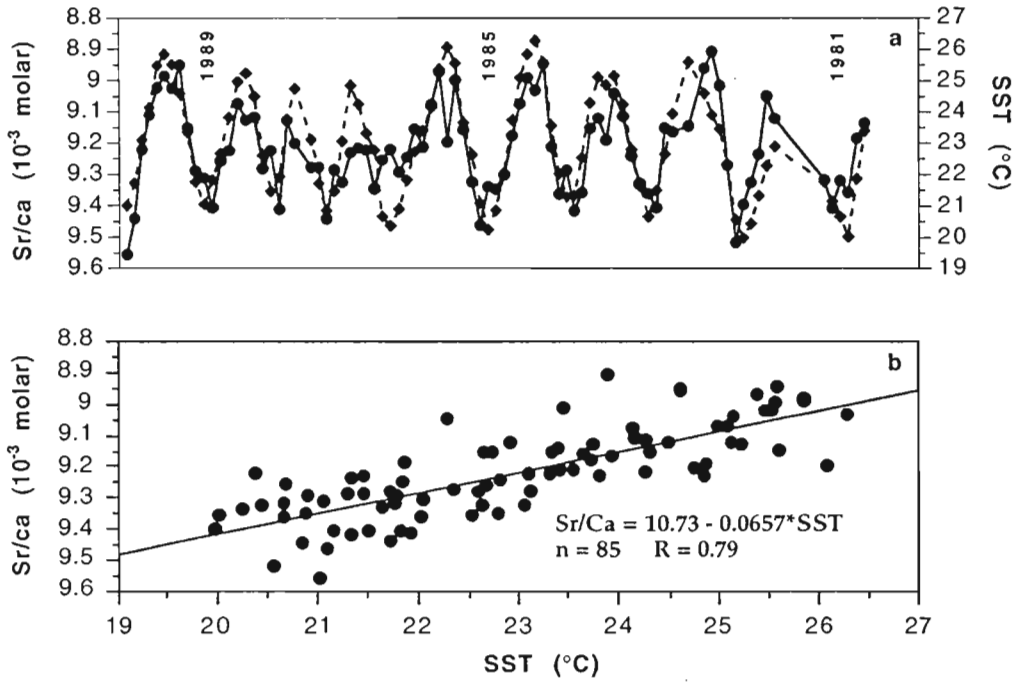

Figure 1. Calibration of the Sr/Ca thermometer in corals: (a) time series of SST (diamonds and dotted line) from Amédée Lighthouse (New Caledonia) and Sr/Ca (dots and solid line) from an adjacent *Porites* coral and (b) regression of Sr/Ca ratios against SST and the resulting equation.

collected at an altitude of +4.66 m above sea level [*Cabioch et al.*, 1998]. Owing to the calculated uplift rate the paleodepth of the *Porites* can be estimated ~ 10-15 m at 4150 years B.P. The surrounding coral assemblages indicate an open shallow marine environment (for details, see *Cabioch et al.*, [1998]). Sr/Ca and U/Ca analyses were converted to SST, using the abovementioned equations. In > 98% of the samples analyzed, Sr and U reconstructed SST agree well within

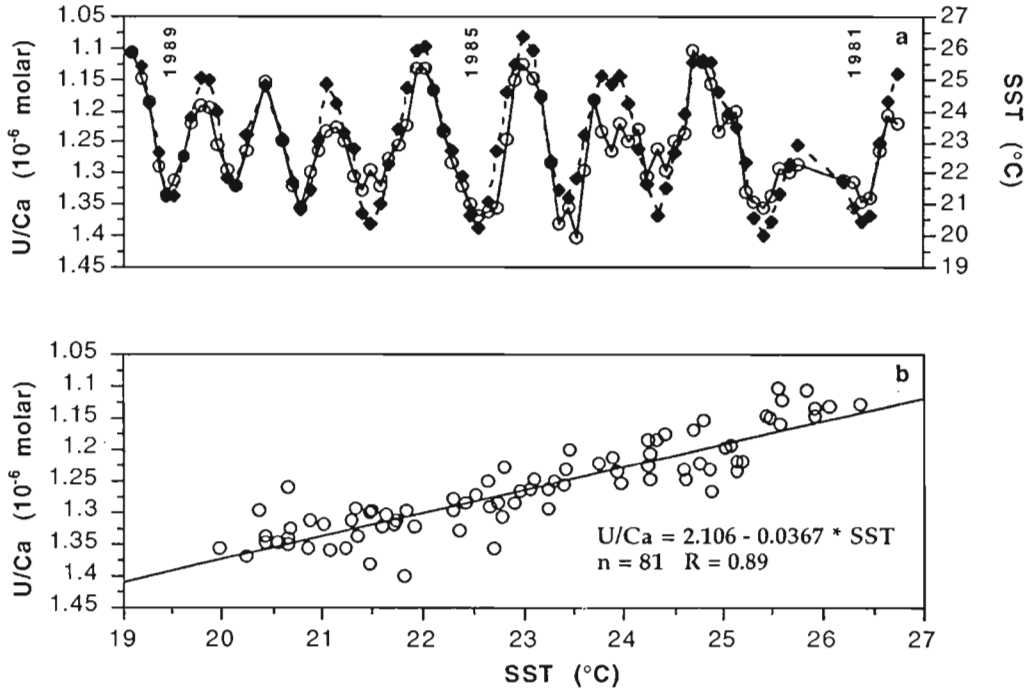

Figure 2. Calibration of the U/Ca thermometer in corals: (a) time series of SST (diamonds and dotted line) from Amédée Lighthouse (New Caledonia) and U/Ca (circles and solid line) from an adjacent *Porites* coral and (b) regression of U/Ca ratios against SST and the resulting equation.

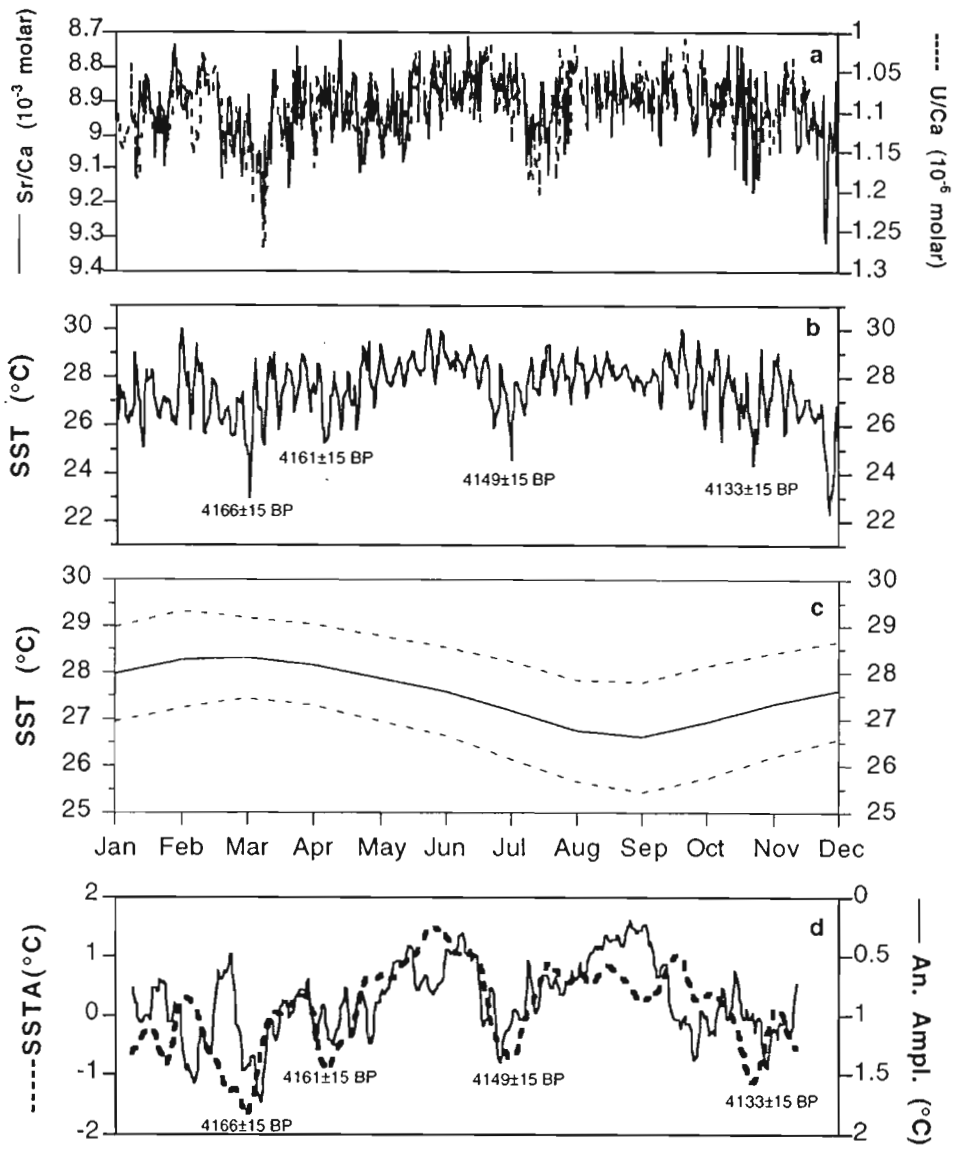

Figure 3. Mid-Holocene coral-derived SST data. (a) Raw time series of the Sr/Ca (solid line) and U/Ca (dashed line) data used to reconstruct the paleo-SST. (b) Composite SST record derived from the Sr/Ca and U/Ca analyses and resampled at monthly intervals. The ages are based on a U/Th date (taken from *Beck et al.*, [1997]). (c) Mean monthly SST (solid line) plus and minus the associated mean monthly standard deviation (dashed lines). (d) Monthly SSTA (dashed line) with respect to the 47-year period average SST (data are filtered with a 25-month Hanning filter) and 24-month running annual amplitude (solid line).

error. The potential effect of Sr/Ca change of seawater through time on the Sr thermometer in coral discussed by *Stoll and Schrag* [1998] does not appear to affect our Vanuatu record since there is a good agreement between the Sr and U reconstructed SST. A 47-year-long composite SST curve was then constructed, and monthly SST values were extrapolated using the Analyseries program (Figure 3)[1]

3. Modern Instrumental Record

The general surface circulation pattern in the southwest Pacific Ocean can be described as a large-scale anticyclonic gyre centered near 15°S [see *Delcroix and Hénin*, 1989, p. 791]. North of this latitude, a westward surface geostrophic flow tends to bring cooler water, whereas south of 15°S, an eastward flow carries warmer water. During an El Niño event the center of the gyre is shifted southward by few degrees of latitude, and Vanuatu is then affected by stronger than average westward flow [*Wyrtki and Wenzel*, 1984; *Delcroix and Hénin*, 1989]. Vanuatu is located on the southwestern fringe of the oceanic domain notably affected by SST changes associated with ENSO [*Delcroix*, 1998]. To assess the exact in-

[1] Supporting data for Figure 3b are electronically archived at World Data Center-A for Paleoclimatology, NOAA/NGDC, 325 Broadway, Boulder, CO 80303. (e-mail: paleo@mail.ngdc.noaa.gov ; URL : http://www.ngdc.noaa.gov/paleo)

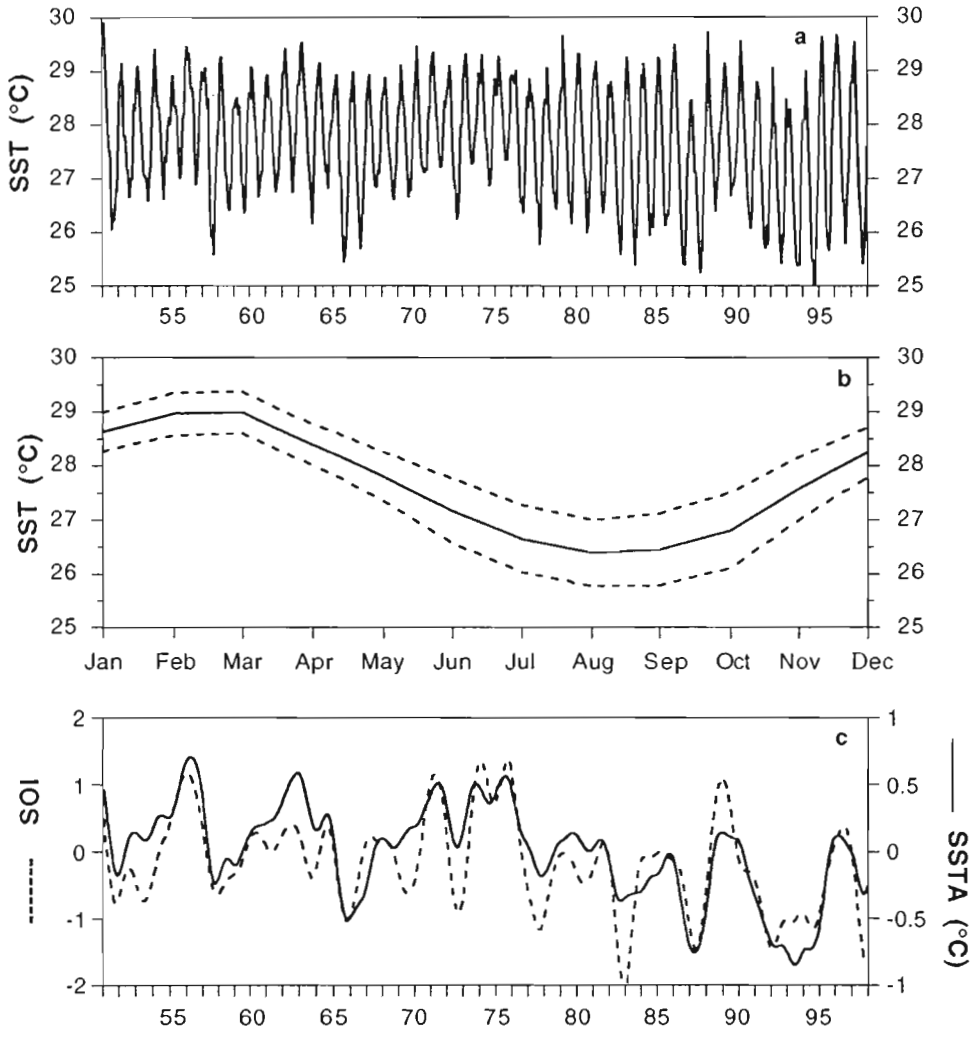

Figure 4. Modern Sea Surface Temperature (SST) data. (a) Monthly 1951-1997 SST for a 1° latitude by 1° longitude box centered on 16°S and 167°E, near Espiritu Santo, Vanuatu, SW Pacific Ocean. (b) Mean monthly SST (solid line) plus and minus the associated mean monthly standard deviation (dashed lines). This graph is plotted with the same scale as Figure 3c for comparison purposes. (c) Comparison of the Southern Oscillation Index (SOI; dashed line) with the monthly SST anomalies (SSTA; solid line) with respect to the 1951-1997 average (27.7°C). Both variables are filtered with a 25-month Hanning filter.

fluence of ENSO on this region, we first looked at the monthly 1951-1997 SST averaged over a 1° latitude by 1° longitude box containing Espiritu Santo [*Reynolds and Smith*, 1994] (Figure 4a). The mean SST for that period is 27.7°C, with a standard deviation of 1.1°C, an annual harmonic amplitude of 1.3°C, and an associated phase of 67°(Figure 4b). We applied a 25-month Hanning filter [*Blackman and Tukey*, 1958] in order to eliminate signals at periods of 1 year or shorter and clearly highlight interannual variations [see *Delcroix*, 1998, Figure 1]. The resulting filtered SST anomalies can then be compared to a filtered Southern Oscillation Index (SOI)(Figure 4c). The two signals are positively correlated (R= 0.80 at zero-month lag) and indicate that ENSO can account for ~64% of the interannual variance of SST. During the warm phase of ENSO [El Niño], SST tends to be colder in Vanuatu, consistent with stronger than average westward flow; sea level drops [see *Delcroix*, 1998, plate 5a], and so do the thermocline shoals, resulting in higher seasonal variability in SST at this latitude. During the cold phase of ENSO (La Niña), the deeper thermocline results in a weak seasonal SST amplitude.

Although quite high, the correlation between the SOI and the SSTA in Vanuatu clearly highlights the complexity of the coupled atmosphere/ocean system and the nonlinear response of SST to changes in the SOI. Spectral analysis of the monthly SST time series (using the Analyseries program [*Paillard et al.*, 1996]) indicate that significant peaks are present in the 2-4-year and 6.5-7-year bands, which are the classical ENSO period [*Enfield and Cid*, 1991]. Sea surface salinity (SSS, results not shown) anomalies also correlate well with the SOI, reinforcing our confidence that Vanuatu is a pertinent area to document ENSO variability through time.

4. Mid-Holocene Coral Record

The mid-Holocene SST record from Vanuatu also strongly exhibits ENSO-like periodicity. This paleo-SST record starts in 4175 ±15 B.P. and ends in 4128 ±15 B.P. (Figure 3). The raw paleo-SST were resampled at monthly intervals assuming

that maximum SST occurred, on average, in March and minimum SST occurred in September as it does today (Figure 4b). However, the maximum of insolation at 16°S happened in November-December at 4150 calendar years B.P., compared to December-January today [*Berger*, 1978], and there is a possibility that the seasonal SST cycle was shifted 1 month backward. In spite of this probable small phase shift we have elected to present the annual harmonic cycle in the paleo-SST record as if it has the same phase as the modern record (Figure 3c). Over the 47-year-long period shown in Figure 3b, the mean SST is 27.6°C with a standard deviation of 1.2°C and an annual harmonic amplitude of 0.8°C (Figure 3c). This mean temperature is very similar to the modern 47-year regional average (27.7°C). Interestingly, the annual harmonic amplitude is somewhat smaller than the modern record (1.3°C). Parts of the paleorecord exhibit a seasonal range significantly larger than in the modern record, while in other portions the range is considerably smaller. A 24-month running annual amplitude (Figure 3d) clearly highlights the strong modulation of the annual cycle through time. This amplitude modulation explains the relatively large standard deviation observed in the paleorecord (Figure 3c). This large interannual variability is highlighted in the paleorecord by several long-lasting cooling events similar to the one at 4166±15 calendar years B.P. described previously [*Beck et al.*, 1997]. When passed through a 25-month Hanning filter, the fossil record yields interannual SST anomalies (Figure 3d) which are 2-3 times greater than seen in the modern period. The two records on Figure 3d are relatively well correlated, suggesting a common mechanism for these variations. Spectral analysis of the fossil SST record reveal periods in the 2-4 and 5.5-6-year bands, which are essentially the same as the dominant modern ENSO peaks.

5. Discussion and Conclusions

Comparison of the modern and fossil records emphasizes the stronger interannual variability which existed at circa 4150 calendar years B.P. Interestingly, this variability occurred at a time when the overall climate is thought to be very similar to the present-day one (same mean SST, similar solar radiation, and no ice volume effect). It is therefore important to determine whether the large interannual cooling events are caused by purely climatic (i.e., the ocean/atmosphere couple) or external factors. One possible external cause for cool SST are volcanic eruptions [*Bradley*, 1988]. The southwest Pacific and Vanuatu, in particular, are tectonically and volcanically active places [*Pelletier et al.*, 1998], and it has been shown recently [*Crowley et al.*, 1997] that coral-derived SST is a good recorder of volcanism. However, cooling events of the magnitude seen in our paleorecord at 4166, 4149, 4133 and 4128 calendar years B.P. (all dates given ±15 years; see Figure 3b) would require volcanic eruptions so large that their signature would certainly be found elsewhere around the globe (for example, the Pinatubo eruption in 1991 caused sea surface temperature anomalies (SSTA) of only 0.5°C in the Western Pacific Warm Pool [*Gagan and Chivas*, 1995]). In particular, sulfate peaks would be present in the polar ice core records. The detailed record of sulfate concentration in the Greenland Ice Sheet Project (GISP) 2 ice core [*Zielinski et al.*, 1994] only documents one peak at ~ 4157 calendar years B.P., which could correlate with either the 4166±15 or the 4149±15 B.P. cooling events. The other cold snaps, however, cannot be explained by volcanism.

By analogy to the modern instrumental record, it could then be argued that the fossil SST record documents a succession of long-lasting La Niña-like to average (i.e., SOI = 0) conditions, interrrupted by strong El Niño-like events. It is likely that during the mid-Holocene the southward (northward) shift of the large-scale anticyclonic gyre center during El Niño (La Niña) resulted in a shoaling (deepening) of the thermocline and a decrease (increase) of the annual amplitude in SST, as seen today. Still, the El Niño of 1982-1983 and 1986-1987 caused SST anomalies (filtered data) of the order of 0.5°C at Vanuatu. Cooling anomalies of 1°C or more, like those seen in the fossil record, imply large-scale oceanic changes not experienced in recent times. In particular, the strong modulation of the SST annual cycle would indicate that the depth of the thermocline and the associated zonal geostrophic circulation fluctuated more extensively than today on an interannual basis. The cause for these large fluctuations is unclear, but although the record is only 47-years-long, a visual inspection of Figures 3b and 3d clearly points to a decadal-scale variability. The three major cooling events (at 4166±15 B.P., 4149±15 B.P., and 4133±15 B.P.) are 17 and 16 years apart, respectively. The occurrence of a 14-17-year periodicity in Pacific coral oxygen isotopic records of the last centuries is now well established [*Dunbar et al.*, 1994; *Linsley et al.*, 1994; *Quinn et al.*, 1996]. On land, it has been identified in laminated sediments from an Ecuadorian lake [*Rodbell et al.*, 1999], where it shows maximum spectral density in the last 1000 years and between ~3000 and 4000 B.P., and in a global surface temperature data set [*Ghil and Vautard*, 1991]. However, reliable modern instrumental SST records are not long enough to fully document the interdecadal mode and its spatial distribution in the Pacific Ocean. Despite this limitation, several authors have proposed that the interdecadal mode could significantly modulate the ENSO cycle [*Holbrook and Bindoff*, 1997; *Latif et al.*, 1997; *Zhang et al.*, 1997; *Gu and Philander*, 1997; *Weaver*, 1999]. A recent simulation [*Weaver*, 1999] which used an extension of the delayed oscillator model showed that extratropical subduction of cooler water which propagates toward the equator [*Gu and Philander*, 1997] could alter ENSO on decadal to interdecadal timescales. This model generates SST time series for the eastern Pacific which mirror well our paleorecord, with significant changes in the seasonal amplitude through time. What we see in the fossil record could then represent phase shifts in the ENSO mode quite similar to those which occurred in the twentieth century [*Zhang et al.*, 1997] but perhaps with stronger exchanges between the tropics and extratropics.

Acknowledgments. We thank Jocelyne Bonneau, Dany Bouttefort, Claude Ihily, Yvan Join, Michel Lardy, and Jean Louis Laurent for help during the course of this work. We also thank Didier Paillard and Henning Kuhnert for help with the use of the Analyseries program. Amy Clement , John Chappell, Richard Grove, and Michael Evans made fruitful comments on an earlier version of this manuscript. We thank our two reviewers, Christina Gallup and George Philander, for their relevant comments. This work was supported by IRD (formely ORSTOM).

References

Alibert, C., and M.T. McCulloch, Strontium/calcium ratios in modern *Porites* corals from the Great Barrier Reef as a proxy for sea surface temperature: Calibration of the thermometer and monitoring of ENSO, *Paleoceanography, 12*, 345-363, 1997.

Beck, J.W., R.L. Edwards, E. Ito, F.W. Taylor, J. Récy, F. Rougerie, P. Joannot, and C. Hénin, Sea-surface temperature from coral skeletal strontium/calcium ratios, *Science, 257*, 644-647, 1992.

Beck, J.W., J. Récy, F.W. Taylor, R.L. Edwards, and G. Cabioch, Abrupt changes in early Holocene tropical sea durface temperature derived from coral record, *Nature, 385*, 705-707, 1997.

Berger, A., Long-term variations of daily insolation and Quaternary climatic change, *J. Atmos. Sci., 35*, 2362-2367, 1978.

Bevington, P.R., and D.K. Robinson, *Data Reduction and Error Analysis for the Physical Sciences*, McGraw-Hill, New York, 1992.

Blackman, R.B., and J.W. Tukey, *The Measurement of Power Spectra*, Dover, Mineola, N.Y., 1958.

Bradley, R.S., The explosive volcanic eruption signal in Northern Hemisphere continental temperature records, *Clim. Change, 12*, 221-243, 1988.

Cabioch, G., F.W. Taylor, J. Récy, R.L. Edwards, S.C. Gray, G. Faure, G.S. Burr, and T. Corrège, Environmental and tectonic influence on growth and internal structure of a fringing reef at Tasmaloum (SW Espiritu Santo, New Hebrides island arc, SW Pacific), *Spec. Publ. Int. Assoc. Sedimentol., 25*, 261-277, 1998.

Crowley, T.J., T.M. Quinn, F.W. Taylor, C. Hénin, and P. Joannot, Evidence for a volcanic cooling signal in a 335-year coral record from New Caledonia, *Paleoceanography, 12*, 633-639, 1997.

Delcroix, T., Observed surface oceanic and atmospheric variability in the tropical Pacific at seasonal and ENSO timescales: a tentative overview, *J. Geophys. Res., 103*, 18,611-18,633, 1998.

Delcroix, T., and C. Hénin, Mechanisms of subsurface thermal structure and sea surface thermohaline variabilities in the southwestern tropical Pacific during 1979-85, *J. Mar. Res., 47*, 777-812, 1989.

Dunbar, R.B., G.M. Wellington, M.W. Colgan, and P.W. Glynn, Eastern Pacific sea surface temperature since 1600 A.D.: the δ^{18}O record of climate variability in Galapagos corals, *Paleoceanography, 9*, 291-315, 1994.

Enfield, D., and L. Cid, Low-frequency changes in El Niño Southern Oscillation, *J. Clim., 4*, 1137-1146, 1991.

Gagan, M.K., and A.R. Chivas, Oxygen isotopes in western Australian coral reveal Pinatubo aerosol-induced cooling in the western Pacific Wann Pool, *Geophys. Res. Lett., 22(9)*, 1069-1072, 1995.

Ghil, M., and R. Vautard, Interdecadal oscillations and the warming trend in global temperature time series, *Nature, 350*, 324-327, 1991.

Gu, D., and G.H. Philander, Internal climate fluctuations that depend on exchanges between the tropics and extratropics, *Science, 275*, 805-807, 1997.

Guilderson, T.P., and D.P. Schrag, Abrupt shift in subsurface temperatures in the tropical Pacific associated with changes in El Niño, *Science, 281*, 240-243, 1998.

Harrison, D.E., and N.K. Larkin, Darwin sea level pressure 1876-1996: Evidence for climate change?, *Geophys. Res. Lett., 24*, 1779-1782, 1997.

Holbrook, N.J., and N.L. Bindoff, Interannual and decadal temperature variability in the southwest Pacific Ocean between 1955 and 1988, *J. Clim., 10*, 1035-1049, 1997.

Latif, M., R. Kleeman, and C. Eckert, Greenhouse warming, decadal variability, or El Niño? An attempt to understand the anomalous 1990s, *J. Clim., 10*, 2221-2239, 1997.

Le Cornec, F., and T. Corrège, Determination of uranium to calcium and strontium to calcium ratios in corals by Inductively Coupled Plasma Mass Spectrometry, *J. Anal. Atom. Spect.*, 12, 969-973, 1997.

Linsley, B.K., R.B. Dunbar, G.M. Wellington, and D.A. Mucciarone, A coral-based reconstruction of intertropical convergence zone variability over Central America since 1707, *J. Geophys., Res. 99*, 9977-9994, 1994.

Min, R.G., R.L. Edwards, F.W. Taylor, J. Récy, C.D. Gallup, and J.W. Beck, Annual cycles of U/Ca in coral skeletons and U/Ca thermometry, *Geochim. et Cosmochim. Acta, 59*, 2025-2042, 1995.

Paillard, D., L. Labeyrie, and P. Yiou, Macintosh program performs time-series analysis, *Eos Trans. AGU, 77 (39)*, 379, 1996.

Pelletier, B., S. Calmant, and R. Pillet, Current tectonics of the Tonga-New Hebrides region, *Earth Planet. Sci. Lett., 164*, 263, 1998.

Quinn, T.M., T.J. Crowley, and F.W. Taylor, New stable isotope results from a 173-year coral from Espiritu Santo, Vanuatu, *Geophys. Res. Lett., 22*, 3413-3416, 1996.

Reynolds, D., and T. Smith, Improved global sea surface temperature analyses using optimum interpolation, *J. Clim., 7*, 929-948, 1994.

Rodbell, D.T., G.O. Seltzer, D.M. Anderson, M.B. Abbott, D.B. Enfield, and J.H. Newman, An ~15,000-year record of El Niño-driven alluviation in southwestern Ecuador, *Science, 283*, 516-520, 1999.

Runyon, R.P., A. Haber, D.J. Pittenger, and K.A. Coleman, *Fundamentals of Behavioral Statistics*, McGraw-Hill, New York, 1996.

Stoll, H.M., and D.P. Schrag, Effects of Quaternary sea level cycles on strontium in seawater, *Geochim. Cosmochim. Acta, 62(7)*, 1107-1118, 1998.

Trenberth, K.E., and T. J. Hoar, The 1990-1995 El Niño-Southern Oscillation event: Longest on record, *Geophys. Res. Lett. 23*, 57-60, 1996.

Trenberth, K.E., and T. J. Hoar, El Niño and climate change. *Geophys. Res. Lett., 24*, 3057-3060, 1997.

Trenberth, K.E., and J.W. Hurrell, Decadal atmosphere-ocean variations in the Pacific, *Clim. Dyn., 9*, 303-319, 1994.

Weaver, A.J., Extratropical subduction and decadal modulation of El Niño, *Geophys. Res. Lett. 26*, 743-746, 1999.

Wyrtki, K., and J. Wenzel, Possible gyre-gyre interaction in the Pacific Ocean, *Nature, 309*, 538-540, 1984.

Zhang, R.-H., L.M. Rothstein, and A.J. Busalacchi, Origin of upper-ocean warming and El Niño change on decadal scales in the tropical Pacific Ocean, *Nature, 391*, 879-883, 1998.

Zhang, Y., J.M. Wallace, and D.S. Battisti, ENSO-like interdecadal variability: 1900-93, *J. Clim., 10*, 1004-1020, 1997.

Zielinski, G.A., P.A. Mayewski, L.D. Meeker, S. Whitlow, M.S. Twickler, M. Morrison, D.A. Meese, A.J. Gow, and R.B. Alley, Record of volcanism since 7000 B.C. from the GISP2 greenland ice core and implications for the volcano-climate system, *Science, 264*, 948-952, 1994.

W. Beck, NSF Arizona AMS Facility, Department of Physics, University of Arizona, Tucson, AZ 85721.

G. Cabioch, T. Corrège, T. Delcroix, and J. Récy, IRD, BP A5, Noumea, New Caledonia. (correge@noumea.ird.nc)

F. Le Cornec, Laboratoire des Formations Superficielles, IRD, 31 Avenue Varagnat, 93143 Bondy cedex, France.

(received May 18, 1999;
revised March 13, 2000;
accepted March 27, 2000.)

GEOPHYSICAL RESEARCH LETTERS, VOL. 27, NO. 23, PAGES 3897-3900, DECEMBER 1, 2000

A coral $\delta^{18}O$ record of ENSO driven sea surface salinity variability in Fiji (south - western tropical Pacific)

Nolwenn Le Bec, Anne Juillet-Leclerc
Laboratoire des Sciences du Climat et de l'Environnement CEA-CNRS, Gif-sur-Yvette, France

Thierry Corrège
Institut de Recherche pour le Développement, Nouméa, New Caledonia

Dominique Blamart
Laboratoire des Sciences du Climat et de l'Environnement CEA-CNRS, Gif-sur-Yvette, France

Thierry Delcroix
Institut de Recherche pour le Développement, Nouméa, New Caledonia

Abstract. The role of salinity in the dynamics and thermodynamics of El Niño - Southern Oscillation (ENSO) events is increasingly being investigated. However, instrumental records of salinity are scarce and short in the tropical Pacific, and there is a clear need for a reliable salinity proxy to extend our knowledge of ENSO through time. Here, we present 40 years of $\delta^{18}O$ data from a Fiji coral (16°48'S - 177°27'E). The coral $\delta^{18}O$ signal integrates both sea surface temperature (SST) and sea surface salinity (SSS) variations. On a seasonal timescale, $\delta^{18}O$ is mainly driven by SST changes whereas on an interannual ENSO timescale, it is almost exclusively affected by SSS variability. Since interannual fluctuations of SSS are rather well correlated to the Southern Oscillation Index in Fiji, coral $\delta^{18}O$ can be used to reconstruct paleo-salinity data with some level of confidence. This may help for tracking ENSO influences back in time.

Introduction

Much useful work to understand and model ENSO has been done neglecting salinity variations [see the special TOGA Decade *J. Geophys. Res. Oceans* volume in June 1998]. However, it is now well recognized that near-surface salinity changes may play a major role in the mixed layer dynamics and thermodynamics of the western Pacific warm pool [*Lukas and Lindstrom*, 1991, *Vialard and Delecluse*, 1998], a region of enhanced ENSO-related air-sea interactions.

Continuous instrumental records seldom exceed a few decades in the tropics. However the understanding of the tropical ocean and atmosphere requires continuous and century-long records of key climate variables such as sea surface temperature (SST), sea surface salinity (SSS) and rainfall. In this context, massive reef-building corals are increasingly used as natural archives to tentatively provide multicentury climate reconstruction.

The oxygen isotopic composition ($\delta^{18}O$) of coral aragonite skeletons is a function of both SST and $\delta^{18}O_{seawater}$ [*Epstein et al.*, 1953, *McConnaughey*, 1989]. Coral $\delta^{18}O$ has been widely used as a paleothermometer assuming a fairly constant $\delta^{18}O_{seawater}$ value [*Dunbar et al.*, 1994, *Wellington et al.*, 1996, *Charles et al.*, 1997, *Boiseau et al.*, 1998, *Cole et al.*, 2000]. Conversely, in regions where temperature variations are small, the $\delta^{18}O$ of coral has been used to reconstruct changes in $\delta^{18}O_{seawater}$ (and by extension, rainfall variability) [*Cole and Fairbanks*, 1990, *Linsley et al.*, 1994, *Tudhope et al.*, 1995]. In sites where the climatic and environmental setting is more complex, coral $\delta^{18}O$ can reflect a composite signal [*Quinn et al.*, 1996, *Klein et al.*, 1997].

In this paper we present the calibration of a Fiji (south western tropical Pacific ocean, 16°48'S - 177°27'E) coral $\delta^{18}O$ time series against the instrumental climatic record, and validate the robustness of $\delta^{18}O$ as a proxy for salinity.

Climatic and Oceanic Setting

The western Pacific warm pool is characterized by the warmest SST ($\geq 28°C$) in the open ocean. Deep active atmospheric convection is located over the warm pool, and over the Intertropical and South Pacific Convergence Zones (ITCZ and SPCZ; see Figure 1). In these zones, precipitation exceeds evaporation, leading to the occurrence of a "fresh pool" ($SSS \leq 35.0$)[*Delcroix et al.*, 1996]. The fresh pool is limited by a well-marked zonal salinity front located at the eastern edge of the maximal rainfall region in the equatorial band [*Picaut et al.*, 1996]. On a seasonal timescale [*Yan et al.*, 1997], the movements of the warm pool are essentially meridional. The warm pool and the SPCZ move southward and reach Fiji in the austral summer (November to April: rainy season). On an interannual timescale, the eastern edge of the warm pool and the salinity front migrate zonally in the equatorial band [*Picaut et al.*, 1996], in phase with the SOI (Southern Oscillation Index). During El Niño events, the SPCZ tends to merge with the ITCZ, leading to dry conditions in Fiji.

Paper number 2000GL011843.
0094-8276/00/2000GL011843$05.00

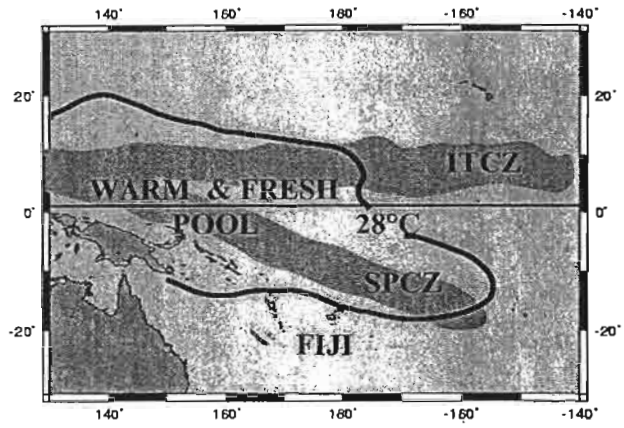

Figure 1. Synthetic map of the western tropical Pacific Ocean. The mean position of the 28°C surface isotherm indicates the margin of the western Pacific warm pool. The mean position of the Intertropical Convergence Zone (ITCZ) and South Tropical Convergence Zone (SPCZ) is also shown.

Material and Methods

A massive colony of *Porites sp.* was drilled in Yasawa Island (16°48'S - 177°27'E) on the western side of the Fiji archipelago, in July 1998 during the IRD (Institut de Recherche pour le Développement) Paleofiji cruise. The core (2.6 m long) was retrieved on the external slope of Nadala Bay fringing reef, at a waterdepth of 2 m. We collected an average of 15 samples per annual band along the maximum growth axis. Organic matter and inorganically precipitated aragonite were removed following the procedure described by *Boiseau and Juillet-Leclerc* [1997]. Samples were analyzed with a VG Optima mass spectrometer. The data are expressed in the conventional delta notation relative to the V-PDB (Vienna Pee Dee Belemnite reference standard) [*Coplen*, 1993].

The analytical uncertainty, i.e. the standard deviation calculated from measurements of a carbonate standard, is 0.067 ‰ (2σ and n = 818). Taking into account the intra-sample isotopic variability from replicate measurements, the total uncertainty is 0.082 ‰.

The chronology is based on peak matching between $\delta^{18}O$ and trace elements data (not shown) on one hand and on instrumental SST on the other hand. The age model uncertainty is ± 1 month. Monthly $\delta^{18}O$ data were extrapolated using the AnalySeries software [*Paillard et al.*, 1996].

To calibrate the coral $\delta^{18}O$ signal, we used monthly SST [*Reynolds and Smith*, 1994], SSS [*Delcroix*, 1998] and rainfall [*Xie and Arkin*, 1996] averaged in a 2°-latitude by 10°-longitude grid centered on 16°S-175°E.

Results and Discussion

We first compared the coral $\delta^{18}O$ to the regional SST (Figure 2A). Both records display a marked seasonality. The regression of the monthly resolved $\delta^{18}O$ record against SST yields the following equation:

$$\delta^{18}O_{coral} = -0.174\ (\pm 0.009)\ SST - 0.032\ (\pm 0.253)\ r = 0.62 \quad (1)$$

Since only 38% of the $\delta^{18}O$ variance is due to SST, the $\delta^{18}O$ signal must also be affected by change in the isotopic composition of the water ($\delta^{18}O_{seawater}$) induced by the precipitation vs. evaporation mass balance and/or by oceanic advection. In Fiji, the effects of SST and net freshwater flux are combined: high (low) SST and rainy (dry) season are concomitant, leading to low (high) coral $\delta^{18}O$ values.

Over the 1960-1998 period, the average SSS annual amplitude is very small (less than 0.2). However, notable interannual variations are clearly visible in Figure 2B. To remove the seasonal component and highlight the inter-annual variability in SSS, $\delta^{18}O$ and SST, the three records were filtered using a 25-month Hanning filter [*Blackman and Tukey*, 1958, *Delcroix*, 1998]. Maximum interannual anomalies (from peak to peak) are 0,77°C, 0,96 and 0,60 ‰ respectively for SST, SSS and $\delta^{18}O_{coral}$. SST isotopic effect on $\delta^{18}O_{coral}$ is relatively weak whereas SSS isotopic effect on $\delta^{18}O_{coral}$ is quite substantial (Figure 3), indicating

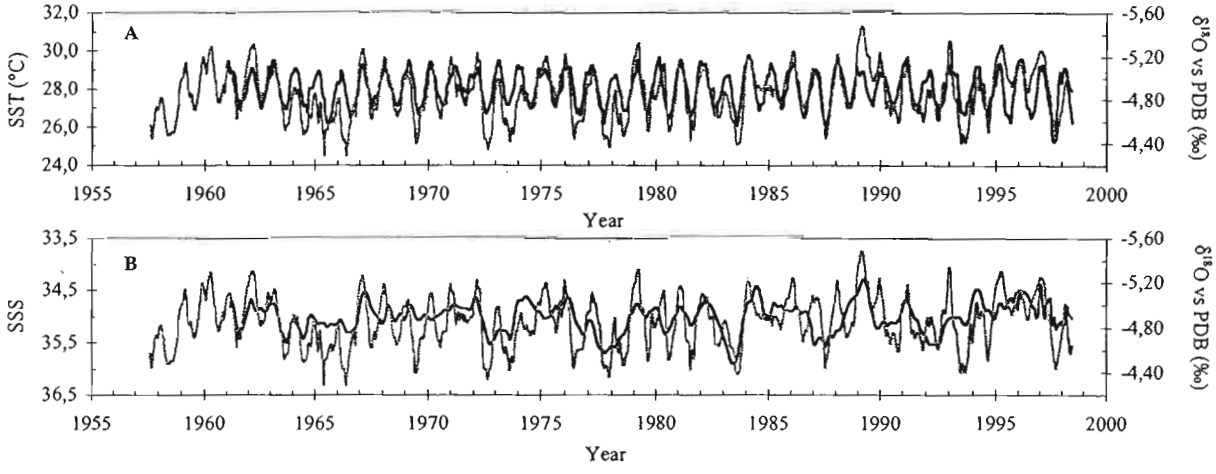

Figure 2. Coral $\delta^{18}O$ record (light line) compared to SST (A) and SSS (B) (dark lines) monthly time series from the Fiji area (see text). The $\delta^{18}O$ scale is conventionally reversed, and so is the SSS scale for easier reading. These are observed time series at zero lag.

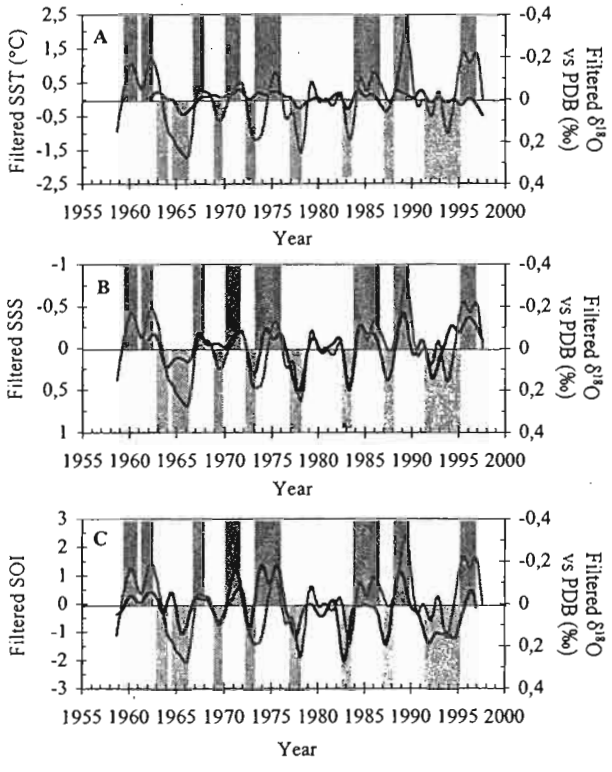

Figure 3. 25-month Hanning filtered time series of $\delta^{18}O$ (light line), SST (A), SSS (B), and SOI (C) (dark lines). $\delta^{18}O$, SST and SSS data are normalized to the 1960-1997 period. The light shaded bars represent El Niño events and the dark shaded ones, La Niña events. The scales of SST and SSS are represented in such a way to express their respective effects on $\delta^{18}O$. These are observed time series at zero lag.

that SSS is the major factor affecting the interannual $\delta^{18}O$ fluctuations (Figure 3B).

The Yasawa coral $\delta^{18}O$ records all the salinity anomalies related to major El Niño and La Niña events since the early 1960's (Figure 3B-C). During El Niño events (light shaded bars on Figure 3) the SPCZ shifts equatorward: rainfall deficit and large evaporation due to wind reinforcement lead to severe droughts and high SSS in Fiji [*Delcroix and Hénin,* 1989]. Thus El Niño events are characterized by positive SSS and coral $\delta^{18}O$ anomalies. During La Niña events (dark shaded bars on Figure 3) the SPCZ migrates southward to Fiji, leading to negative SSS and coral $\delta^{18}O$ anomalies. Zonal advections induced by the displacement of the subtropical gyre center during the ENSO cycle may also contribute to changes in SST and SSS [*Delcroix and Hénin*, 1989, *Corrège et al.*, 2000]. It is worth noting that the SST interannual variability, although quite small in amplitude, is also linked to the ENSO cycle with a tendency for slightly lower (higher) SST developing during El Niño (La Niña) events (Figure 3A).

Table 1 summarizes the relationship between the SOI and the interannual anomalies in coral $\delta^{18}O$, SST, SSS, rainfall. These are rather well correlated to the SOI, the usual atmospheric index for basin-scale ENSO signal.

A notable result is the rather good correlation (r = 0.71) between SSS and $\delta^{18}O_{coral}$. It clearly indicates that $\delta^{18}O_{coral}$ can be used as a proxy for reconstructing salinity variability on an interannual timescale in the studied region. We then calculated the relationship linking the $\delta^{18}O_{coral}$ and SSS interannual variations using the filtered data:

$$\delta^{18}O_{coral} = 0.428\ (\pm 0.020)\ SSS - 19.843\ (\pm 0.722)\quad r=0.71 \quad (2)$$

The slope of this line (s = 0.428 ± 0.020) is close to the slope (s = 0.384 ± 0.008) of the $\delta^{18}O_{seawater}$ vs. SSS calibration calculated in the Fiji area using the method developed by *Delaygue et al.* [2000]. In this latter study the $\delta^{18}O_{seawater}$ is simulated using the OPA oceanic general circulation model [*Madec et al.*, 1998] where the atmospheric fluxes are prescribed by the isotopic version of the NASA/GISS atmospheric model [*Jouzel et al.*, 1987]. This result from a model reinforces our observational conclusion that the Yasawa coral $\delta^{18}O$ is a reliable tracer of seawater $\delta^{18}O$ interannual variations, and consequently of salinity.

To conclude, we have shown that in the Fiji area, where ENSO driven interannual variations in SST are small compared to SSS variations, the $\delta^{18}O$ record of massive corals can be used as a reliable tool to track salinity anomalies back in time. Given the present-day ENSO influence on SSS, this feature may prove useful for inferring regional past ENSO variability. We are now extending the $\delta^{18}O$ record of the Fiji coral to the beginning of the century, together with Sr/Ca measurements as a temperature proxy. We will also generate similar records from other ENSO sensitive areas such as Tuvalu and Tokelau.

Table 1. Summary of Correlation Coefficients (r Values) Between the Coral $\delta^{18}O$ Record and the Climatic Records (all Data are Filtered with a 25-month Hanning Filter). Correlations are Significant at the 95% Confidence Level.

	SOI	Rainfall	SST	SSS
Rainfall	0.58	...	...	...
SST	0.64	0.75	...	...
SSS	-0.62 *	-0.67 *	-0.47	...
coral $\delta^{18}O$	-0.45 *	-0.41 *	-0.41	0.71

* denotes that a 3-month lag time was introduced, the SOI or rainfall preceding the SSS and coral $\delta^{18}O$ signals by 3 months.

Acknowledgments. This work was supported by the IRD program "Climate Variability and Regional Impacts" and Paléocéan Project. We thank Jacques Récy, leader of the Paléocéan Project, and Guy Cabioch, leader of the Paleofiji cruise. We are most thankful to the officers and crew of the IRD R/V Alis. Guy Cabioch, Yvan Join, Joël Orempüller and Stéphanie Reynaud-Vaganay provided assistance in coral drilling. Jocelyne Bonneau helped for the sample collection. The SURTROPAC / ECOP group at IRD Nouméa was instrumental in collecting in situ SSS data from voluntary observing ships for three decades. We express our gratitude to the Government of Fiji for allowing us to work in their economic zone. We also thank Michael Evans and an anonymous reviewer for their relevant comments. This is LSCE contribution number 0514.

References

Blackman, D.S., and J.W. Tukey, *The measurement of Power Spectra,* 190pp., Dover, Mineola, N.Y., 1958.

Boiseau, M., and A. Juillet-Leclerc, H_2O_2 treatment of recent coral aragonite: oxygen and carbon isotopic implications, *Chem. Geol., 143*, 171-180, 1997.

Boiseau, M., A. Juillet-Leclerc, P. Yiou, B. Salvat, P. Isdale, and M. Guillaume, Atmospheric and oceanic evidences of ENSO events in central Pacific Ocean from stable coral isotopic records over the last 137 years, *Paleoceanography, 13* (6), 671-685, 1998.

Charles, C.D., D.E. Hunter, and R.G. Fairbanks, Interaction between the ENSO and the Asian monsoon in a coral record of tropical climate, *Science, 277*, 925-928, 1997.

Cole, J.E., R.B. Dunbar, T.R. McClanahan, and N.A. Muthiga, Tropical Pacific forcing of decadal SST variability in the Western Indian Ocean over the past two centuries, *Science, 287*, 617-619, 2000.

Cole, J.E., and R.G. Fairbanks, The Southern Oscillation recorded in the $\delta^{18}O$ of corals from Tarawa atoll, *Paleoceanography, 5* (5), 669-683, 1990.

Coplen, T.B., Reporting of stable carbon, hydrogen and oxygen isotopic abundances. *In: Reference and intercomparison materials for stable isotopes light elements, Int. At. Energy Agency, Tech. Doc. 825*, pp. 31-38, Vienna, 1993.

Corrège, T., T. Delcroix, J. Récy, J.W. Beck, G. Cabioch, and F. Le Cornec, Evidence for stronger ENSO events in a mid-Holocene massive coral, *Paleoceanography, 15* (4) 465-470, 2000.

Delaygue G., J. Jouzel, and J.C. Dutay, Oxygen 18 - Salinity relationship simulated by an oceanic general circulation model, *EPSL, 178*, 113-123, 2000.

Delcroix, T., and C. Hénin, Mecanisms of subsurface thermal structure and sea-surface thermohaline variabilities in the south-western tropical Pacific during 1979-1985, *J. Mar. Res., 47*, 777-812, 1989.

Delcroix, T., Observed surface oceanic and atmospheric variability in the tropical Pacific at seasonal and ENSO timescales: a tentative overview., *J. Geophys. Res., 103*, 18611-18633, 1998.

Delcroix, T., C. Hénin, V. Porte, and P. Arkin, Precipitation and sea-surface salinity in the tropical Pacific Ocean., *Deep Sea Res. I*, 43, 1123-1141, 1996.

Dunbar, R.B., G.M. Wellington, M.W. Colgan, and P.W. Glynn, Eastern Pacific sea surface temperature since 1600 A.D.: the $\delta^{18}O$ record of climate variability in Galapagos corals, *Paleoceanography, 9* (2), 291-315, 1994.

Epstein, S., R. Buchsbaum, H. Lowenstam, and H.C. Urey, Revised carbonate-water isotopic temperature scale, *Bull. Geol. Soc. Am., 62*, 417-425, 1953.

Jouzel, J., G.L. Russel, R.J. Suozzo, R.D. Koster, J.W.C. White, and W.S. Broecker, Simulations of the HDO and $H_2^{18}O$ atmospheric cycles using the NASA GISS General Circulation Model: the seasonal cycle for present-day conditions, *J. Geophys. Res., 92*, 14739-14760, 1987.

Klein, R., A.W. Tudhope, C.P. Chilcott, J. Pätzold, A. Z., M. Fine, A.E. Fallick, and Y. Loya, Evaluating southern Red Sea corals as a proxy record for the Asian monsoon, *Earth Planet. Sci. Let., 148*, 381-394, 1997.

Linsley, B.K., R.B. Dunbar, G.M. Wellington, and D.A. Mucciarone, A coral-based reconstruction of intertropical convergence zone variability over Central America since 1707, *J. Geophys. Res., 99* (C5), 9977-9994, 1994.

Lukas, R., and E. Lindstrom, The mixed layer of the western equatorial Pacific Ocean, *J. Geophys. Res., 96*, 3343-3358, 1991.

Madec, G., P. Delecluse, M. Imbard, and C. Lévy, OPA 8.1 ocean general circulation model reference manual, *Notes du Pôle de modélisation*, IPSL, 1998. (PDF-version available at: http://www.ipsl.jussieu.fr/modelisation/notes/OPA8.1-Total.pdf)

McConnaughey, T., C-13 and O-18 isotopic disequilibria in biological carbonates: I. Patterns, *Geochim. and Cosmochim. Acta, 53*, 163-171, 1989.

Paillard D., L. Labeyrie, and P. Yiou, Macintosh program performs time-series analysis, *Eos Trans. AGU*, 77, 379, 1996. (An electronic supplement of this reference is available at: http://www.agu.org/eos_elec/96097e.html)

Picaut, J., M. Ioualalen, C. Menkes, T. Delcroix, and M.J. McPhaden, Mechanism of the zonal displacements of the Pacific warm pool, implications for ENSO, *Science, 274*, 1486-1489, 1996.

Quinn, T.M., T.J. Crowley, and F.W. Taylor, New stable isotope results from a 173-year coral from Espiritu Santo, Vanuatu, *Geophys. Res. Lett., 23* (23), 3413-3416, 1996.

Reynolds, D., and T. Smith, Improved global sea surface temperature analyses using optimum interpolation, *J. Clim., 7*, 929-948, 1994.

Tudhope, A.W., G.B. Shimmield, C.P. Chilcott, M. Jebb, A.E. Fallick, and A.N. Dalgleish, Recent changes in climate in the far western equatorial Pacific and their relationship to the Southern Oscillation; oxygen isotope records from massive corals, Papua New Guinea, *Earth Planet. Sci. Let., 136*, 575-590, 1995.

Vialard, J., and P. Delecluse, An OGCM study for the TOGA decade. Part I : Role of salinity in the physics of the western Pacific fresh pool, *J. Phys. Oceanogr., 28*, 1071-1088, 1998.

Wellington, G.M., R.B. Dunbar, and G. Merlen, Calibration of stable oxygen isotope signatures in Galapagos corals, *Paleoceanography, 11* (4), 467-480, 1996.

Xie, P., and P. Arkin, Analyses of global monthly precipitation using gauge observations, satellite estimates, and numerical model predictions, *J. Clim., 9*, 840-858, 1996.

Yan, X.-H., Y. He, W. T. Liu, Q. Zheng, and C.-H. Ho, Centroid movement of the western Pacific warm pool during the three recent El Niño-Southern Oscillation events, *J. Phys. Oceanogr., 27*, 837-845, 1997.

D. Blamart, A. Juillet-Leclerc, N. Le Bec, Laboratoire des Sciences du Climat et de l'Environnement, CEA-CNRS, 91198 Gif sur Yvette cédex, France. (e-mail: Nolwenn.Le-bec@lsce.cnrs-gif.fr)

T. Corrège, T. Delcroix, Institut de Recherche pour le Développement, BP A5, Nouméa, New Caledonia.

(Received June 5, 2000; accepted October 12, 2000)

GEOPHYSICAL RESEARCH LETTERS, VOL. 28, NO. 18, PAGES 3477-3480, SEPTEMBER 15, 2001

Little Ice Age sea surface temperature variability in the southwest tropical Pacific

Thierry Corrège[1], Terry Quinn[2], Thierry Delcroix[1], Florence Le Cornec[3], Jacques Récy[1] and Guy Cabioch[1]

Abstract. We present a 60-year near-monthly record of tropical sea surface temperature (SST) during the Little Ice Age derived from coupled Sr/Ca and U/Ca analysis of a massive coral from New Caledonia (southwest tropical Pacific). The record indicates that, from 1701 to 1761, surface temperatures were on average 1.4°C cooler than during the past 30 years. This cooling was accompanied by strong interannual to interdecadal oscillations that changed the background state. Correlations between SST changes and the Southern Oscillation and the Pacific Decadal Oscillation are evolutive and appear to depend on the background state.

Introduction

The climate of the Pacific zone is mostly under the influence of El Niño Southern Oscillation (ENSO) events. As longer records of ENSO-related sea surface temperature (SST) changes become available and theoretical and modelling studies progress, the role of the background state of the ocean/atmosphere system is increasingly being acknowledged (Philander, 1999; Lau and Weng, 1999). Understanding how interdecadal and long-term variations in the background climate state affect the phasing and strength of ENSO is thus a necessary step to improve climate predictions (Timmerman et al., 1999 ; Barnett and Latif, 2000 ; Collins, 2000). Here, we report on a 60 year record of coral-derived monthly SST from the south-western tropical Pacific during the early eighteenth century. This period lies in the heart of the Little Ice Age (LIA; ~1400-1850 A.D.), an era of documented cooler climate in mid-latitudes (Bradley and Jones, 1993) and in the tropical Atlantic Ocean (Keigwin, 1996 ; Winter et al., 2000), which precedes the industrial revolution and associated increase in greenhouse gases. Our aim is twofold: 1.) Search for a possible cooling of surface waters associated with the LIA in the southwestern tropical Pacific Ocean and 2.) If any, evaluate how such a cooling affected climate variability at interannual (i.e. ENSO) to interdecadal time scale.

[1]Institut de Recherche pour le Développement, BP A5, 98848 Nouméa, New Caledonia
[2] College of Marine Science, University of South Florida, 140 Seventh Avenue South, MSL 119, St. Petersburg, Florida 33701, USA
[3]Institut de Recherche pour le Développement, 32 Avenue Varagnat, 93143 Bondy cedex, France

Paper number 2001GL013216.
0094-8276/01/2001GL013216$05.00

Methods and Data

The coral we used is a portion of a large colony of Porites cf. lutea collected near Amédée Lighthouse (New Caledonia; 22°30' S, 166°30' E; subsequently AL). Coral slabs were sampled and trace elements analyses were performed according to procedures described elsewhere (Le Cornec and Corrège, 1997; Corrège et al., 2000). Both Sr/Ca and U/Ca ratios are well correlated to modern-day instrumental SST at AL (Corrège et al., 2000) and can be used with confidence to infer past SST. For each pseudo monthly sample, Sr/Ca and U/Ca gave paleo-SST estimates that were averaged and extrapolated to derive a composite monthly SST record (Fig. 1). These monthly SST were then passed through a 25-month and a 169-month Hanning filter (Blackman and Tukey, 1958) respectively to highlight interannual and interdecadal SST variability. Oxygen and carbon isotopes were measured previously at a resolution of 4 samples per year on the whole colony (Quinn et al., 1998), which started to grow circa 1657 A.D. (Fig. 2). We chose to perform high-resolution analyses (12 samples per year) of trace elements on the first 60 years of the eighteenth century because this period encompasses the coldest years of the last 350 years according to oxygen isotopes (Fig. 2). The interest of trace elements is that, whereas the oxygen isotopic record of corals is integrative of both temperature and isotopic composition (and hence, salinity) of surface water (Gagan et al., 1998), trace elements can provide an almost pure temperature signal (Beck et al., 1992; Alibert and McCulloch, 1997). The combined use of Sr and U, which are incorporated in corals at different ratios with respect to temperature, is a guarantee of the robustness of the SST reconstruction.

Results and Discussion

At present, ENSO events induce a signature in the vicinity of New Caledonia (Delcroix and Lenormand, 1997) which consists in colder than average SST during the warm phase (i.e. El Niño) of ENSO, and in warmer than average SST during the cold phase (i.e. La Niña). Correlation of the SST anomaly (SSTA) at AL with the Southern Oscillation Index (SOI) is about 0.6, and is maximum when the SOI precedes the SSTA by three months (Delcroix and Lenormand, 1997). For the last 30 years, the mean SST at AL is 23.4°C (based on daily bucket measurements), with a maximum peak to trough (i.e. La Niña to El Niño) amplitude of interannual SST anomaly reaching ~1.5°C.

The original oxygen isotopic data indicates a gradual warming from the XVIIIth century to the present (see Table 1 and Fig. 2). However, cooler SST are often linked to drier conditions in New Caledonia, yielding to positive $\delta^{18}O$ anomalies

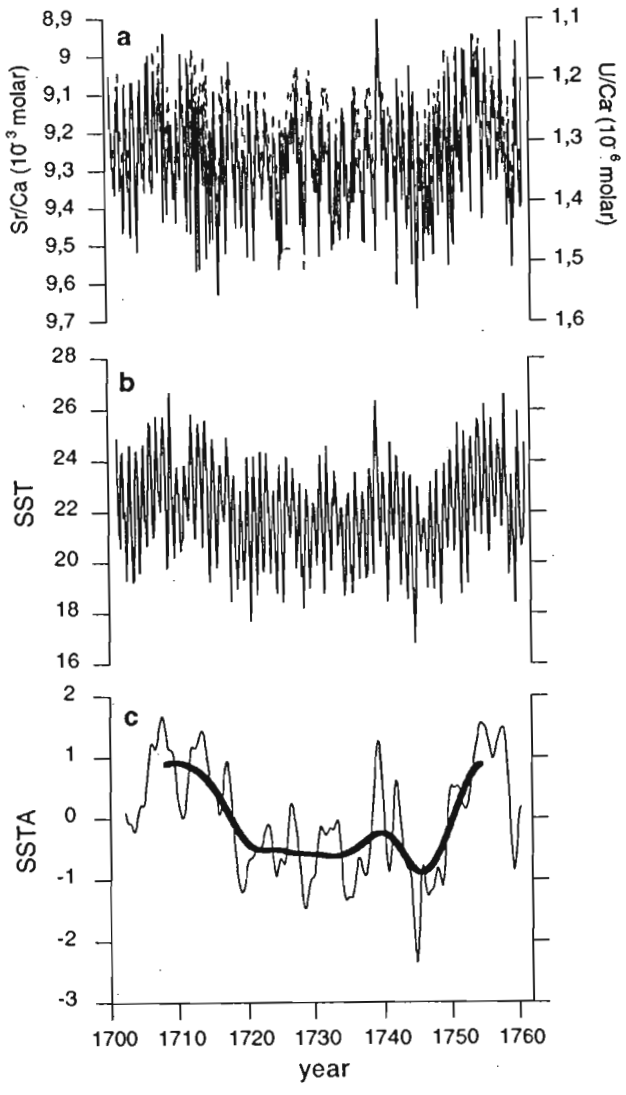

Figure1. Reconstructed Sea Surface Temperature (SST) at Amédée Lighthouse between 1701 and 1761 AD; **a**: Raw times series of Sr/Ca (solid line) and U/Ca (dashed line) analyses; **b**: Composite monthly SST record derived from Sr/Ca and U/Ca analyses. In each sample, both trace element ratios were converted to SST following the equations presented in Corrège et al. (2000), and then averaged. The whole series was then resampled at monthly intervals; **c**: Interannual (thin line) and interdecadal (thick line) monthly SST anomalies with respect to the 60-year period average SST. Anomalies were calculated by applying respectively a 25-month (for interannual anomalies) and a 169-month (for interdecadal anomalies) Hanning filter to the monthly SST.

resulting in reconstructed SST which would be too cold. The coral trace element data indeed indicate that the mean SST from 1701 to 1761 was 22°C, as opposed to 21.6°C given by the $\delta^{18}O$. This represents a cooling of ~1.4°C with respect to the last 30 years. The paleo-record from AL also indicates a strong interdecadal SST modulation, with the lowest SST between 1720 and 1740 being ~2°C colder than present day values (Fig. 1). This drop in SST is consistent with the 1°C cooling derived from planktonic foraminifers for the LIA in the Sargasso Sea (Keigwin, 1996), and with the 2° to 3°C cooling measured in Caribbean corals of similar age (Winter et al., 2000).

Although part of the cooling described by the long $\delta^{18}O$ record can be attributed to a change in the isotopic composition of surface water, it can be nonetheless concluded that the southwestern Pacific in the vicinity of New Caledonia was cooler during part of the LIA. The spatial extension of this cooling is difficult to assert, but at present, low frequency SST changes at any point in the southwest Pacific can be extrapolated with confidence over about 4-6° of latitude and 10-15° of longitude (Meyers et al., 1991). Coral records from the Great Barrier reef and from Panama also show cooler and/or drier conditions prior to 1850, but other corals from the central and eastern south Pacific record no obvious trend (see Gagan et al., 2000 for a synthesis).

The coral record from AL also delivers valuable information about interannual (ENSO) to interdecadal variability in pre-industrial times. The fact that three of the four coolest episodes on record (namely 1720, 1728 and 1747-48, see Fig. 1) are rated as strong to very strong El Niño years in documentary evidence from South America (Ortlieb, 2000) provides additional proofs of the robustness of our coral record. The coldest year on record in the studied period (1744)

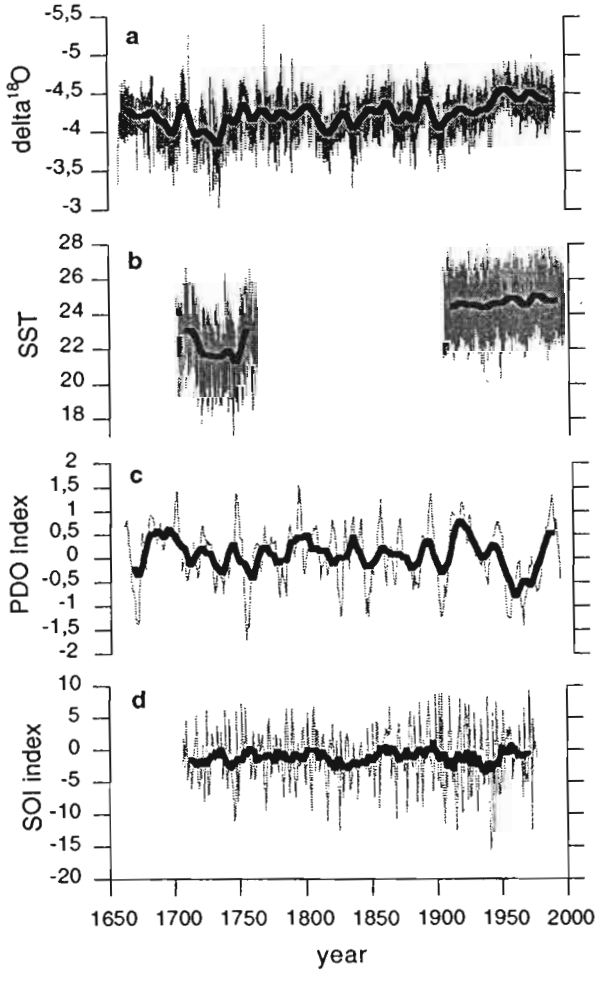

Figure 2. **a**: Times series of Amédée Lighthouse oxygen isotopes (Quinn et al., 1998); **b**: regional SST from 1903-1993 (GISST2.2 data from the GOSTA plus CD-ROM) and reconstructed AL SST from 1701-1761; **c**: reconstructed PDO index (Biondi et al., 2001); **d**: reconstructed northern hemisphere winter (DJF) SOI index (Stahle et al., 1998). Thick lines represent interdecadal trend (see text).

Table 1. Instrumental and reconstructed mean SST at Amédée Lighthouse over several time intervals; $\delta^{18}O$ SST calculated with RMA equation and quarterly ORSTOM SST from Quinn et al., 1998; ORSTOM SST from daily bucket SST measurements; GISST2.2 from GOSTA plus CD-ROM. These are regional SST; TE: Trace elements.

Period	$\delta^{18}O$ SST	ORSTOM SST	GISST2.2	TE SST
1967-1993	23.5°C	23.4°C	24.7°C	
1903-1993	23.0°C		24.5°C	
1801-1900	22.2°C			
1701-1800	21.8°C			
1701-1761	21.6°C			22.0°C

is potentially identified as an El Niño year (Ortlieb, 2000), but is also affected by a cooling caused by a major volcanic eruption (Crowley et al., 1997). When the strong interdecadal SSTA (clearly highlighted by the 169-month filter; see Fig. 1) is taken as a baseline, it appears that interannual SSTA from 1701 to 1761 are similar to modern values, and are of the order of 0.5°C to 1.5°C, implying no change in the regional ENSO signature. This is consistent with the model results indicating that pre-industrial CO_2 levels have at least to be multiplied by four (i.e. twice as much as the present-day value) before any change in ENSO frequency or amplitude can be detected (Collins, 2000). Spectral analysis of the 1701-61 SST record did not identify significant spectral peaks, but the recurrence of negative SSTA linked to El Niño at AL still lies in the typical ENSO band of 2 to 7 years (Fig. 1).

To further investigate ENSO behavior in colder times, we compared the December to February (DJF) SOI derived from tree rings (Stahle et al., 1998) to the March to May (MAM) Amédée SST (to account for the three-month lag present today). The two records are statistically correlated (R=0.35, significant at 1% level). However, close examination of the records indicates that the correlation evolves with time. To visualize this tendency, we took a sliding window of 15 years and calculated the correlation coefficient for each block (assigned to the mid point of the period) (Fig. 3). During the warmest periods (pre-1720 and post 1735), SST and the SOI are well correlated. During the coldest period (~1720-1735), there is no correlation between the SST at AL and the DJF SOI. This raises the possibility that the western Pacific warm pool cooled below 28°C, which constitute an important temperature threshold for organized atmospheric convection. In that case, the generation of ENSO events could be seriously altered (Philander, 1990, 1999). However, interannual SSTA are still present in the coral record during this period, and El Niño events are documented in Peru (Ortlieb, 2000). If these SSTA are indeed ENSO-related, then the reliability of the SOI proxy might be altered when backgound conditions get cooler in the western Pacific. Alternatively, the AL SSTA could have been generated by a phenomenon other than ENSO yet to be determined.

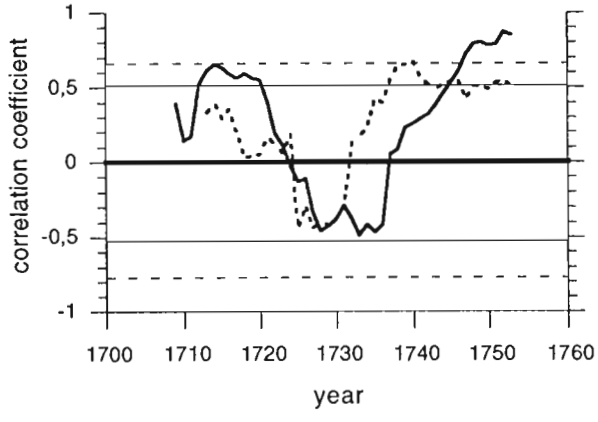

Figure 3. Correlation coefficients between mean annual SST at Amédée Lighthouse and the reconstructed SOI (dashed line) and PDO (solid line) records for 15-year overlapping subperiods (see text for reference of records). For each subperiod, the calculated correlation coefficient was assigned to the mid point. The length of the subperiods was chosen to highlight interdecadal variability. Results are not significantly altered by choosing slightly different subperiod length. Full and dashed horizontal lines represent 5% and 1% significance levels respectively. For the correlation with the northern hemisphere winter (DJF) reconstructed SOI, the mean of three months of Amédée Lighthouse SST (namely March, April and May) was used.

In addition to the interannual signal, the AL SST record contains a strong interdecadal component (Fig. 1), as opposed to the XXth century instrumental record (Fig. 2). This is consistent with the findings of Urban et al. (2000) who reported stronger decadal cycles in the tropical Pacific during part of the XIXth century, when background conditions were cooler. The coral SST series from AL is too short to identify unambiguously any spectral peak in the interdecadal band, but Quinn et al. (1998) did identify a marginally significant (92-94%) peak around 14.3 to 15.4 years in their quarterly isotopic record. Is this interdecadal variability linked to the Pacific (inter) Decadal Oscillation (PDO; Mantua et al., 1997) and involves exchanges between high and low latitudes? Recently, Biondi et al. (2001) proposed an annual reconstruction of the PDO based on tree rings from the southwestern part of America, which extends back to 1661. Comparison of the AL SST record (annual means) with this PDO indicates an overall good correlation between the two records (R=0.45, significant at 1% level). The evolutive correlation is shown on Fig. 3. During the warmest periods, the modern-day pattern is present, i.e. mean SST raise at AL when the PDO is negative. When SST is at its lowest the relationship seems to reverse. This result emphasizes the fact that, as pointed out elsewhere (Alverson et al., 2001), more data and better spatial coverage are needed before we can fully understand how interactions between the tropics and higher latitudes can drive climate change on decadal timescales.

Acknowledgements. We thank F. Taylor, Y. Join and B. Pelletier for collecting the Amédée coral core, and Pascal Yiou for performing spectral analysis on our record. This article was greatly improved by reviews from W. Beck, Y. Gouriou and two anonymous reviewers, and by comments from Yves M. Tourre. Data other than our own were provided by the WDC-A for Paleoclimatology and the UK Met Office. This work was supported by IRD and NSF. Supporting data will be archived at the WDC-A for Paleoclimatology.

References

Alibert, C., and M.T. McCulloch, Strontium/calcium ratios in modern *Porites* corals from the Great Barrier Reef as a proxy for sea surface temperature : calibration of the thermometer and monitoring of ENSO. *Paleoceanography, 12*, 345-363, 1997.

Alverson, K., G.W.K. Moore, G. Holdsworth, and J.E. Cole, Improving climate predictability and understanding decadal

variability using proxy climate data. *CLIVAR Exchanges, 6(1),* 4-5, 2001.

Barnett, T.P., and M. Latif, Connections between the Pacific Ocean tropics and midlatitudes on decadal timescale. *J. Clim. 13,* 1173-1194, 2000.

Beck, J.W., R.L. Edwards, E. Ito, F.W. Taylor, J. Récy, F. Rougerie, P. Joannot and C. Hénin, Sea-surface temperature from coral skeletal strontium/calcium ratios. *Science 257,* 644-647, 1992

Biondi, F., A. Gershunov, and D.R. Cayan, North Pacific decadal climate variability since 1661. *J. Clim. 14,* 5-10, 2001.

Blackman, D.S., and J.W. Tukey, *The measurement of Power Spectra*, 190pp., Dover, Mineola, N.Y., 1958.

Bradley, R.S., and P.D. Jones, 'Little Ice Age' summer temperature variations: their nature and relevance to recent global warming trends. *The Holocene 3,* 367-376, 1993.

Collins, M., The El Niño-southern oscillation in the second Hadley Centre coupled model and its response to greenhouse warming. *J. Clim. 13,* 1299-1312, 2000.

Corrège, T., T. Delcroix, J. Récy, J.W. Beck, G. Cabioch, and F. Le Cornec, Evidence for stronger ENSO events in a mid-Holocene massive coral, *Paleoceanography 15*, 465-470, 2000.

Crowley, T.J., T.M. Quinn, F.W. Taylor, C. Hénin, and P. Joannot, Evidence for a volcanic cooling signal in a 335-year coral record from New Caledonia. *Paleoceanography, 12,* 633-639, 1997.

Delcroix, T., and O. Lenormand, ENSO signals in the vicinity of New Caledonia, South Western Pacific. *Oceanol. Acta 20,* 481-491, 1997.

Gagan, M.K., L.K. Ayliffe, D. Hopley, J.A. Cali, G.E. Mortimer, J. Chappell, M.T. McCulloch, and M.J. Head, Temperature and surface-ocean water balance of the mid-Holocene tropical western Pacific. *Science 279,* 1014-1018, 1998.

Gagan, M.K., L.K. Ayliffe, J.W. Beck, J.E. Cole, E.R.M. Druffel, R.B. Dunbar, and D.P. Schrag, New views of tropical paleoclimates from corals. *Quat. Sc. Rev. 19,* 45-64, 2000.

Keigwin, L.D., The Little Ice Age and medieval warm period in the Sargasso Sea. *Science 274,* 1504-1508, 1996.

Lau, K.M., and H. Weng, Interannual, decadal-interdecadal, and global warming signals in sea surface temperature during 1955-97. *J. Clim. 12,* 1257-1267, 1999.

Le Cornec, F., and T. Corrège, Determination of uranium to calcium and strontium to calcium ratios in corals by Inductively Coupled Plasma Mass Spectrometry. *J. Anal. Atom. Spect. 12,* 969-973, 1997.

Mantua, N.J., S.R. Hare, Y. Zhang, J.M. Wallace, and R.C. Francis, A Pacific interdecadal climate oscillation with impacts on salmon production. *Bull. Am. Meteorol. Soc. 78,* 1069-1079, 1997.

Meyers G., H. Phillips, N. Smith, and J. Sprintall, Space and time scales for optimal interpolation of temperature - tropical Pacific ocean. *Progr. Oceanogr., 28,* 189-218, 1991

Ortlieb, L., The documentary historical record of El Niño events in Peru: An update of the Quinn record (sixtennth through nineteenth centuries). in El Niño and the Southern Oscillation: Variability, Global and Regional Impacts, H. Diaz & V. Markgraf (Eds.), Cambridge University Press, 207-295, 2000

Philander, S.G., *El Niño, La Niña and the Southern Oscillation.* Academic Press, NY, 1990

Philander, S.G., A review of tropical ocean-atmosphere interactions. *Tellus, 51 A-B,* 71-90, 1999

Quinn T.M., T.J. Crowley, F.W. Taylor, C. Hénin, P. Joannot, and Y. Join, A multi-century stable isotope record from a New Caledonia coral: interannual and decadal sea surface temperature variability in the southwest Pacific since 1657 A.D. *Paleoceanography, 13,* 412-426, 1998.

Stahle, D.W., R.D. D'Arrigo, P.J. Krusic, M.K. Cleaveland, E.R. Cook, R.J. Allan, J.E. Cole, R.B. Dunbar, M.D. Therrell, D.A. Gay, M.D. Moore, M.A. Stokes, B.T. Burns, J. Villanueva-Diaz, and L.G. Thompson, Experimental dendroclimatic reconstruction of the southern oscillation. *Bull. Am. Meteor. Soc. 79,* 2137-2152, 1998.

Timmermann, A., J. Oberhuber, A. Bacher, M. Esch, M., Latif, and E. Roeckner, Increased El Niño frequency in a climate model forced by future greenhouse warming. *Nature 398,* 694-696, 1999.

Urban, F.E., J.E. Cole, and J.T. Overpeck, Influence of mean climate change on climate variability from a 155-year tropical Pacific coral record. *Nature, 407,* 989-993, 2000.

Winter, A., H. Ishioroshi, T. Watanabe, T. Oba, and J. Christy, Caribbean sea surface temperatures: two-to-three degrees cooler than present during the Little Ice Age. *Geophys. Res. Lett. 27,* 3365-3368, 2000.

G. Cabioch, Th. Corrège, Th. Delcroix, and J. Récy, Institut de Recherche pour le Développement, BP A5, 98848 Nouméa, New Caledonia (e-mail : correge@noumea.ird.nc)

F. Le Cornec, Institut de Recherche pour le Développement, 32 Avenue Varagnat, 93143 Bondy cedex, France

T. Quinn, College of Marine Science, University of South Florida, 140 Seventh Avenue South, MSL 119, St. Petersburg, Florida 33701, USA

(Received March 23, 2001 ; revised: July 16, 2001 ; accepted: July 17, 2001)

Centre IRD de Nouméa
B.P. A5 Nouméa Cédex, 98848, Nouvelle-Calédonie